Acta Pharmaceutica Sinica B 2024;14(2):579–601

Chinese Pharmaceutical Association
Institute of Materia Medica, Chinese Academy of Medical Sciences

Acta Pharmaceutica Sinica B

www.elsevier.com/locate/apsb
www.sciencedirect.com

REVIEW

Lipid nanovehicles overcome barriers to systemic RNA delivery: Lipid components, fabrication methods, and rational design

Jing Yan[a,b,†], Hao Zhang[a,c,†], Guangfeng Li[d,†], Jiacan Su[a,c,e,*], Yan Wei[a,e,*], Can Xu[f,*]

[a]*Institute of Translational Medicine, Shanghai University, Shanghai 200444, China*
[b]*Institute of Medicine, Shanghai University, Shanghai 200444, China*
[c]*Department of Orthopedics, Xinhua Hospital, Shanghai Jiao Tong University School of Medicine, Shanghai 200092, China*
[d]*Department of Orthopedics, Shanghai Zhongye Hospital, Shanghai 200941, China*
[e]*Organoid Research Center, Shanghai University, Shanghai 200444, China*
[f]*Department of Gastroenterology, Changhai Hospital, Shanghai 200433, China*

Received 17 July 2023; received in revised form 24 September 2023; accepted 8 October 2023

KEY WORDS

Lipid nanovehicles;
RNA therapeutics;
Barriers to systemic RNA delivery;
Lipid components;
Fabrication methods;
Lipid nanovehicle design;
Extrahepatic tissue targeting;
Organ tropism

Abstract Lipid nanovehicles are currently the most advanced vehicles used for RNA delivery, as demonstrated by the approval of patisiran for amyloidosis therapy in 2018. To illuminate the unique superiority of lipid nanovehicles in RNA delivery, in this review, we first introduce various RNA therapeutics, describe systemic delivery barriers, and explain the lipid components and methods used for lipid nanovehicle preparation. Then, we emphasize crucial advances in lipid nanovehicle design for overcoming barriers to systemic RNA delivery. Finally, the current status and challenges of lipid nanovehicle-based RNA therapeutics in clinical applications are also discussed. Our objective is to provide a comprehensive overview showing how to utilize lipid nanovehicles to overcome multiple barriers to systemic RNA delivery, inspiring the development of more high-performance RNA lipid nanovesicles in the future.

© 2024 The Authors. Published by Elsevier B.V. on behalf of Chinese Pharmaceutical Association and Institute of Materia Medica, Chinese Academy of Medical Sciences. This is an open access article under the CC BY-NC-ND license (http://creativecommons.org/licenses/by-nc-nd/4.0/).

*Corresponding authors.
E-mail addresses: xucan@smmu.edu.cn (Can Xu), ywei@shu.edu.cn (Yan Wei), drsujiacan@163.com (Jiacan Su).
[†]These authors made equal contributions to this work.

Peer review under the responsibility of Chinese Pharmaceutical Association and Institute of Materia Medica, Chinese Academy of Medical Sciences.

https://doi.org/10.1016/j.apsb.2023.10.012
2211-3835 © 2024 The Authors. Published by Elsevier B.V. on behalf of Chinese Pharmaceutical Association and Institute of Materia Medica, Chinese Academy of Medical Sciences. This is an open access article under the CC BY-NC-ND license (http://creativecommons.org/licenses/by-nc-nd/4.0/).

1. Introduction

In human disease treatment, conventional antibodies or small-molecule drugs cannot effectively target numerous pathogenic proteins[1]. In contrast, RNA-based therapeutics, *e.g.*, small interfering RNAs (siRNAs), short hairpin RNAs (shRNAs), microRNAs (miRNAs), and messenger RNAs (mRNAs), can regulate the expression of a protein by silencing specific genes or encoding related proteins. Therefore, RNAs introduce new treatment possibilities for otherwise undruggable human diseases[2]. Despite their unique advantages, naked RNAs do not readily lead to desirable outcomes after systemic injection due to RNAs undergoing rapid filtration through the kidney, enzymatic degradation, and phagocytosis by macrophages in the circulatory system and generally low cellular internalization[3,4]. Thus, the main challenge for those establishing RNA therapeutics is the construction of safe and effective vehicles for overcoming multiple delivery barriers.

For systemic RNA delivery, carrier systems fall into viral and nonviral vectors. Most clinical trials to date have evaluated the use of viral vehicles. However, only 4.2% of these viral vectors have been evaluated in patients at a late clinical stage due to their undesirable immunogenicity and general toxicity[5]. Therefore, nonviral vectors, especially lipid nanovehicles, are garnering intensive attention by virtue of their lower immunogenicity and higher safety than those of viral vehicles, ability to encapsulate large payloads, and ease of manufacturing[6−9]. Conventional liposomes used for RNA entrapment were introduced in the late 1970s; however, they showed low encapsulation ability, partly due to neutral lipids and passive encapsulation methods[10]. Later, lipoplexes were developed; they comprise cationic lipids that can form complexes with negatively charged RNAs, leading to efficient RNA encapsulation. However, the constitutively charged cationic lipids caused the lipoplexes to be rapidly eliminated from the circulatory system and to activate the immune system, thereby precluding their use in the clinical. The advent of ionizable lipids made it possible to develop pharmacologically useful lipid formulations[11]. Specifically, pH-titratable lipids are almost entirely uncharged at the physiological pH of blood but positively charged at the acidic pH of endosomes. These features enable these lipid carriers to interact with negatively charged RNAs and endosomal membranes but prevent disadvantageous rapid clearance and low tolerability. Cationic or ionizable lipids with poly (ethylene glycol) (PEG)-lipids and helper lipids constitute the main components of lipid nanovehicles used for RNA delivery. PEG-lipids contribute to drug formulation stability during the production process and can shield the surface of lipid nanovehicles from blood components to optimize their pharmacokinetics and biodistribution. Helper lipids mainly facilitate lipid nanovehicles to escape from endosomes.

With the development of preparation technology, lipid nanovehicles have been developed from conventional lipoplexes to stabilized nucleic acid-lipid particles (SNALPs), lipopolyplexes, membrane/core nanoparticles (MCNPs), and lipid nanoparticles (LNPs). Therefore, in this review, lipid nanovehicles specifically include lipoplexes, SNALPs, lipopolyplexes, MCNPs, and LNPs. In contrast to classical hollow liposomes, lipopolyplexes, MCNPs, and LNPs contain a solid internal core that encapsulates RNA molecules, and therefore, they show higher kinetic stability and more rigid morphology. In particular, homogeneous LNPs are obtained by large-scale commercial fabrication methods such as T-mixing or microfluidic-mixing technology. Accordingly, LNPs are the most advanced lipid nanovehicles to deliver RNAs developed to date[12]. Since 2018, three LNP-based RNA therapeutics have been approved for clinical use, *i.e.*, Alnylam patisiran (ONPATTRO) (a siRNA drug used for the treatment of transthyretin-mediated amyloidosis), Moderna mRNA-1273 (an mRNA vaccine used for the prevention of COVID-19) and Pfizer BNT162b2 (another mRNA vaccine used for the prevention of COVID-19)[13]. Patisiran was the first nonviral vector product to be marketed, validating the applicability of lipid nanovehicles to RNA delivery.

Systemic injection is an ideal route for RNA administration, allowing them to reach target cells more efficiently[14]. Hence, in this review, systemic RNA delivery is mainly discussed. Various types of RNA molecules and multiple barriers to their systemic delivery are first introduced. The functions of lipid nanovehicles depend mainly on their lipid components, including their cationic or ionizable lipids, helper lipids, and PEG lipids; additionally, preparation methods exert profound effects on lipid nanovehicle structures[15], and therefore the effects of both the component and method factors are highlighted. In particular, approaches to rationally designing lipid nanovehicles that overcome the multiple hurdles of systemic RNA delivery are extensively articulated. Finally, the status quo and challenges of lipid nanovehicle-based RNA therapeutics in clinical use are analyzed, and future research directions are proposed. Notably, previously published relevant reviews focused on multiple types of RNA-loaded nanovectors used for cancer treatment[16−18], localized RNA delivery to treat pulmonary diseases[19,20], or LNPs for transporting RNAs, proteins, and small-molecule drugs[21]. In contrast, we mainly discuss a series of lipid nanovehicles (*i.e.*, lipoplexes, SNALPs, LNPs, MCNPs, and lipopolyplexes) and strategies to design lipid nanovehicles that overcome multiple obstacles to systemic RNA delivery (Fig. 1). Overall, we aim to inspire the development of highly efficient lipid nanovehicles that induce low toxicity levels for use in RNA delivery shortly.

2. RNA-based therapeutics

Based on different action mechanisms, RNA-based therapeutics include multiple types, such as siRNAs, shRNAs, and miRNAs. The structural and functional characteristics of these RNAs are summarized in Table 1.

2.1. *Small interfering RNAs and short hairpin RNAs*

RNA interference (RNAi) was first discovered as a natural antiviral defense mechanism in plants[2]. Long double-stranded RNAs (dsRNAs) produced during viral replication can be cleaved by Dicer, an endoribonuclease or helicase with an RNase motif, into 21−23 nucleotide double-stranded siRNAs[22]. Mature siRNAs can also be produced through direct chemical synthesis or by Dicer processing of shRNAs (Fig. 2A). One siRNA strand is called the guide (or antisense) strand. In contrast, the other strand is designated the passenger (or sense) strand. A siRNA binds to multiple proteins to form an RNA-induced silencing complex (RISC) through which the passenger strand is cleaved by the enzyme Argonaute-2 (Ago2). Then, the guide strand attached to the activated RISC directs RISC to target mRNA *via* sequence homology, and Ago2 then cleaves the corresponding mRNA, leading to specific gene silencing.

ShRNAs are synthetic RNA molecules with a short hairpin secondary structure and generally comprise 20−25 nucleotides[23]. Because shRNAs are delivered in a DNA plasmid rather than as

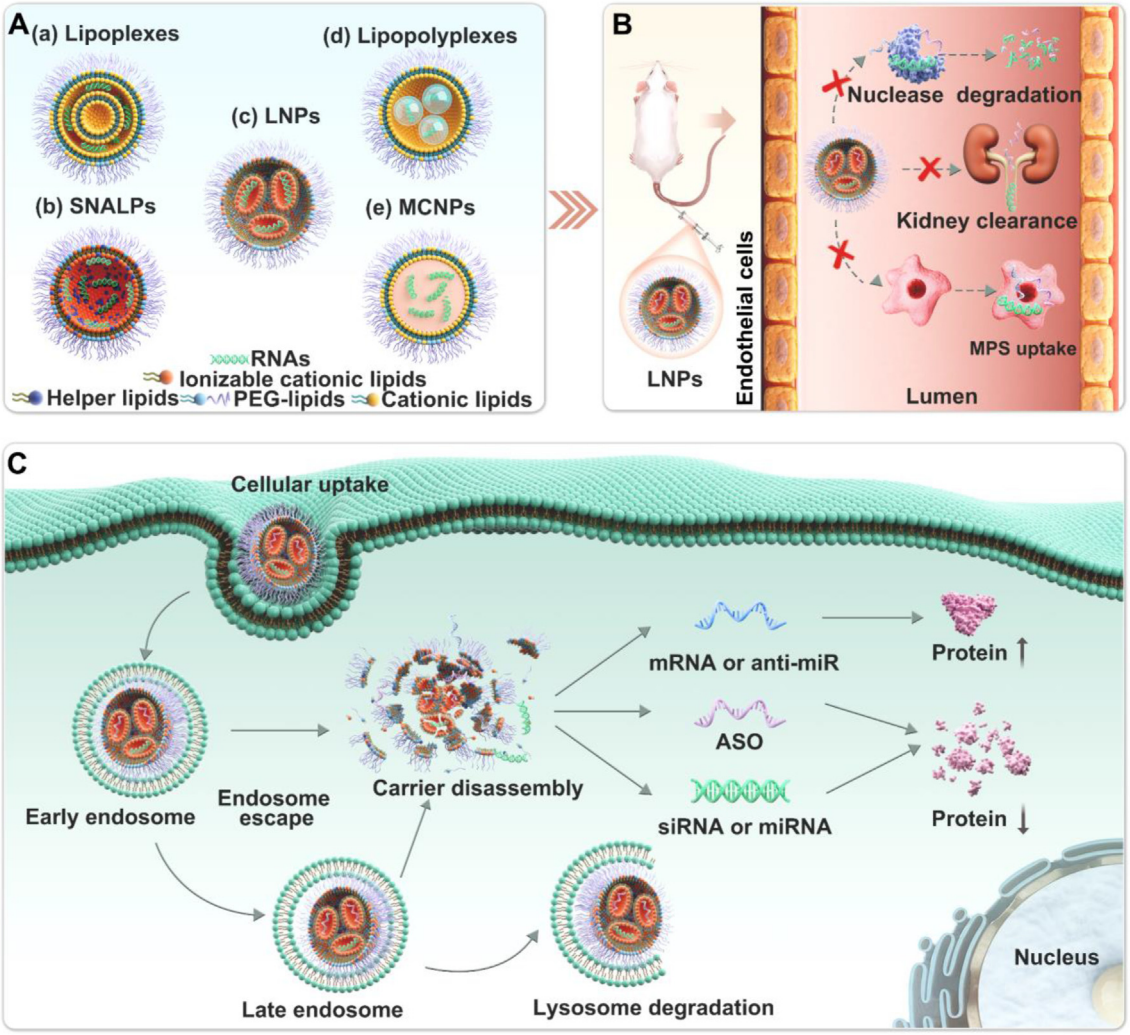

Figure 1 Lipid nanovehicles overcome multiple barriers to systemic RNA delivery. (A) Various lipid nanovehicles, including lipoplexes, stabilized nucleic acid-lipid particles (SNALPs), lipid nanoparticles (LNPs), membrane/core nanoparticles (MCNPs), and lipopolyplexes, are assembled with crucial lipid components. (B) Extracellular barriers: well-designed lipid nanovehicles such as LNPs protect RNAs from nuclease degradation, kidney elimination, and phagocytosis by the mononuclear phagocyte system (MPS) in the circulatory system. (C) Intracellular barriers: well-designed lipid nanovehicles such as LNPs enter target cells, escape from endosomes, and release loaded RNAs into the cytoplasm that ultimately regulate gene expression.

dsRNAs, they can be expressed persistently for months or years (Fig. 2A). After transcription, the product is processed by Drosha to produce pre-shRNA, which then enters the cytoplasm *via* Exportin 5-mediated export. Then, a shRNA is cleaved by Dicer to yield an siRNA that subsequently induces gene silencing.

2.2. *MicroRNAs and microRNA antagonists*

In addition to siRNA and shRNA, RNAi mechanism-based therapeutics include miRNAs and miRNA antagonists (anti-miRs). MiRNAs are noncoding RNAs comprising approximately 22−24 nucleotides. MiRNAs are encoded by endogenous miRNA genes that drive the generation of primary miRNA (pri-miRNA) in the nucleus (Fig. 2B)[24]. Pri-miRNA is then degraded into precursor miRNA (pre-miRNA), exported from the nucleus into the cytosol by Exportin 5, and processed into mature miRNA. Natural mature endogenous miRNA is single-stranded, while chemically synthesized miRNA is typically double-stranded, resulting in higher performance and stability *in vitro* and *in vivo*. When exported into the cytoplasm, synthesized miRNAs are loaded onto RISCs, and the passenger miRNA strand is cleaved, which removes it from the complex. This process activates the RISC, resulting in subsequent gene targeting and silencing *via* either translation repression or mRNA degradation[25].

An anti-miR, a synthetic single-stranded RNA, is entirely complementary to a specific miRNA which suppresses Ago2-mediated cleavage of target miRNA by mismatching at the cleavage site of Ago2 or certain base modifications (Fig. 2C)[26]. Hence, after introducing an anti-miR corresponding to a miRNA, the expression of the gene initially inhibited by the miRNA is upregulated.

Although both siRNAs and miRNAs are noncoding RNAs that can induce gene silencing, their modes of action and clinical potential differ. MiRNAs can modulate the expression of hundreds of genes by base mispairing, while siRNAs exert effects on a single gene at a specific location.

Table 1 Summary of various RNA therapeutics in terms of their structural and functional characteristics.

RNA type	Length	Structure	Action site	Target
siRNA	21−23 nucleotides	Double stranded	Cytoplasm	mRNA
shRNA	20−25 nucleotides	Double stranded with a short hairpin structure	Cytoplasm	mRNA
miRNA	22−24 nucleotides	Double stranded or single stranded	Cytoplasm	mRNA
anti-miR	17−22 nucleotides	Single stranded	Cytoplasm	miRNA
ASO	12−25 nucleotides	Single stranded	Nucleus or cytoplasm	Pre-mRNA or mRNA
saRNA	~21 nucleotides	Double stranded	Nucleus	Pre-mRNA
mRNA	2000−2500 nucleotides	Single stranded	Cytoplasm	N/A

N/A: not available.

2.3. *Antisense oligonucleotides*

Antisense oligonucleotides (ASOs), single-stranded nucleotide sequences, comprise 12−25 nucleotides that can specifically block the transcription or translation of target genes[27]. ASOs regulate gene expression through mRNA degradation or occupancy-only mechanisms. Once bound to an mRNA *via* Watson−Crick base pairing, ASOs form hybrid substrates of endogenous Ribonuclease H1 (RNase H1). RNase H1-induced cleavage at the binding position of an ASO destroys the target mRNA, thereby silencing target protein expression (Fig. 2D)[28]. The cleaved RNA product is then eliminated through regular cellular degradation routes in the cytoplasm or nucleus[29].

In addition, by binding a functional *cis*-element of the target pre-mRNA, ASOs prevent cellular machinery from reaching the pre-mRNAs (Fig. 2E). Therefore, ASOs may induce isoform splice switching and inhibit the translation of mRNA or reduce target mRNA stability, thereby downregulating target protein expression.

2.4. *Small activating RNAs*

In contrast to siRNA- or miRNA-induced gene silencing, chemically synthesized small activating RNAs (saRNAs) can upregulate gene expression. This phenomenon, called RNA activation (RNAa), is a small RNA-directed and Ago2-dependent gene expression modulation process in which short dsRNAs target promoters to enhance the expression of target genes at the transcriptional/epigenetic level (Fig. 2F)[30]. This regulatory process is highly regulated and evolutionarily conserved. Notably, saRNAs are very useful for developing novel treatments against undruggable diseases[31,32].

2.5. *Messenger RNAs*

An mRNA can deliver genetic information from genes to protein synthesis machinery. Therefore, mRNAs are essential to expressing specific encoded proteins and modulation of posttranslational modifications (Fig. 2G)[33]. Notably, mRNA therapy, which involves synthesizing and injecting a specific mRNA into a patient's body, allows cells to generate the target therapeutic proteins *in vivo*, which avoids the massive manufacturing issues related to recombinant proteins. mRNAs function for shorter periods than DNA therapy. Therefore, DNA therapy is suitable for treating inherited diseases caused by genetic mutations, while RNA treatment may be an alternative to treating other diseases.

RNA-based therapeutics provide several unique advantages over conventional antibody and small-molecule drugs. First, RNA therapeutics specifically target a single gene without affecting off-target genes. In contrast, small-molecule drugs frequently exert effects on multiple targets, increasing the possibility for off-target binding of unknown proteins. Second, in contrast to static antibody and small-molecule treatment, RNA-based therapeutics can pharmaceutically evolve their sequence at the same rate as disease progression, such as the progression of pandemic influenza or cancer, thereby facilitating the cure of undruggable diseases. Third, once a delivery system has been developed to transport RNAs to a specific cell type (*e.g.*, delivering siRNAs to hepatocytes), every disease-associated RNA in that cell type is highly likely to achieve targeted delivery.

3. Multiple biological barriers to systemic RNA delivery

Systemic injection is an ideal administration route that enables RNAs to reach target cells more efficiently than other routes[14]. However, multiple extracellular and intracellular barriers severely limit their effective delivery. After injection into the blood, RNAs must first overcome extracellular barriers, including endogenous nuclease-induced degradation, kidney filtration, and uptake by the MPS (Fig. 3A). First, nucleases widely exist in plasma and tissues. The main nuclease in plasma is a 3'−5' exonuclease, and it can also cleave internucleotide-formed bonds. Therefore, RNAs undergo ribozyme degradation in the blood circulatory system[34]. Second, RNAs are rapidly eliminated from the bloodstream through kidney filtration[35]. The pore size of the glomerular filtration barrier is approximately 8 nm[36], which allows molecules <50 kDa to pass through the kidney. Most RNAs have a molecular weight of <50 kDa and thus can pass through glomeruli and into urine. In addition, the MPS is critical for clearing foreign pathogens, cellular debris, and apoptotic cells *via* phagocytosis, and they can engulf many RNAs[37]. The MPS comprises phagocytic cells, including mononuclear phagocytes and tissue macrophages. Tissue macrophages are the most abundant in the liver (Kupffer cells) and spleen. Therefore, RNA molecules show high accumulation levels in these organs after systemic administration.

Furthermore, the cell membrane is a fluid mosaic membrane composed of a uniform anion phospholipid bilayer with randomly floating proteins (Fig. 3B). Small, neutral, and slightly hydrophobic molecules (<1000 Da) can passively cross the lipid bilayer. However, all RNA therapeutics are highly negatively charged macromolecules that cannot pass through the cell membrane[4,18] and thus must enter cells in a specific vehicle.

Lipid nanovehicles are generally taken up *via* endocytosis, which involves diverse pathways, such as caveolae-mediated endocytosis (CvME), clathrin-mediated endocytosis (CME)[38], and macropinocytosis pathways[39]. Therefore, lipid nanovehicle-mediated intracellular transport of RNAs usually begins in early endosomes. During endosomal maturation, the endosomal environment changes from being neutral to being slightly acidic (pH ~6.5 in early endosomes, pH ~5.5 in late endosomes, and pH ~4.7 in lysosomes) (Fig. 3B). In particular, lysosomes contain

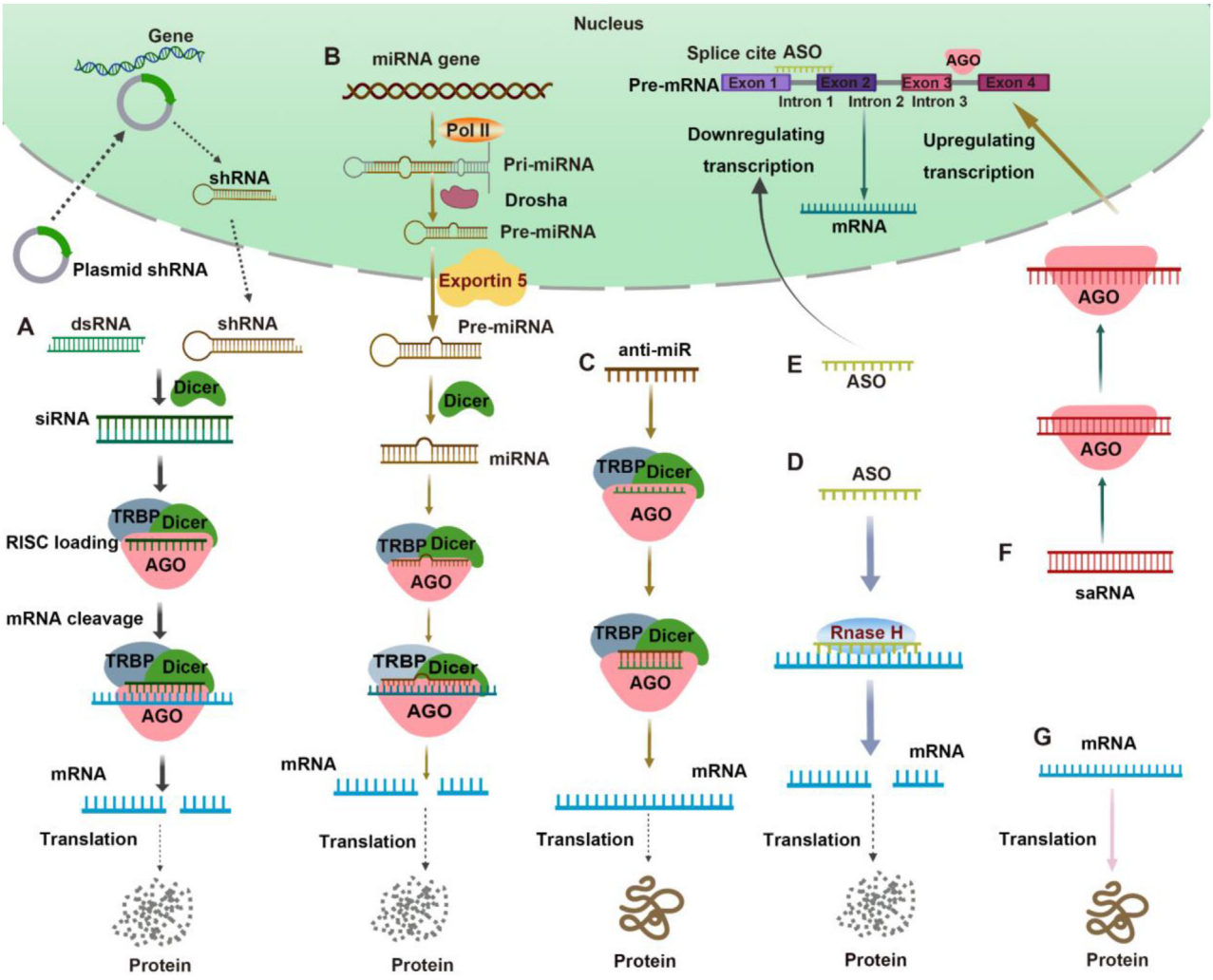

Figure 2 Action mechanisms underlying various RNA-based therapeutics. (A) Short interfering RNAs (siRNAs) and short hairpin RNAs (shRNAs) silence genes when the guide strand is incorporated in an RNA-induced silencing complex RISC) to degrade target messenger RNAs (mRNAs). (B) MicroRNAs (miRNAs) are encoded by endogenous miRNA genes and are synthesized in the nucleus. After entering the cytoplasm, miRNAs silence genes *via* mRNA degradation or translation repression. (C) miRNA antagonists (anti-miRs) upregulate gene expression by matching a specific target miRNA to inhibit its cleavage by Ago2. Antisense oligonucleotides (ASOs) downregulate genes *via* (D) mRNA degradation or (E) occupancy-only mechanisms. (F) Small activating RNAs (saRNAs) target promoters to upregulate target gene expression at the transcriptional level. (G) mRNAs encode specific proteins and modulate posttranslational modifications.

various nucleases that degrade RNAs[40]. Thus, RNAs must escape from endosomes before lysosome formation to avoid enzymatic degradation[41].

4. Lipid components used for constructing lipid nanovehicles

Lipid nanovehicles, extensively used for RNA delivery, comprise three essential components: cationic or ionizable cationic lipids, helper lipids, and PEG lipids. These main lipids are introduced herein based on their chemical structures and functions.

4.1. Cationic lipids

Cationic lipids bear a permanent positive charge on head groups and thus can interact with anionic RNAs *via* electrostatic interactions, promoting their encapsulation during lipid nanovehicle synthesis[42]. Moreover, cationic lipids mediate electrostatic interactions between lipid nanovehicles and the cell and endosomal membrane, conducive to their cellular uptake and endosomal escape, respectively[43]. However, cationic lipids induce cytotoxicity, such as hemolysis and undesirable immune stimulation, and rapid plasma clearance[44].

Based on the chemical structure of their head groups, cationic lipids can be classified into four kinds of lipids: quaternary ammonium, guanidinium, pyridinium and imidazolium lipids (Fig. 4A). Notably, cationic lipids with delocalized positive charges, such as imidazolium, pyridinium and guanidinium, show less cytotoxicity than quaternary ammonium lipids.

4.1.1. Quaternary ammonium lipids

Since the 1980s, many types of cationic lipids with quaternary ammonium head groups have been synthesized for the delivery of DNAs or RNAs; these include 1,2-di-*O*-octadecenyl-3-

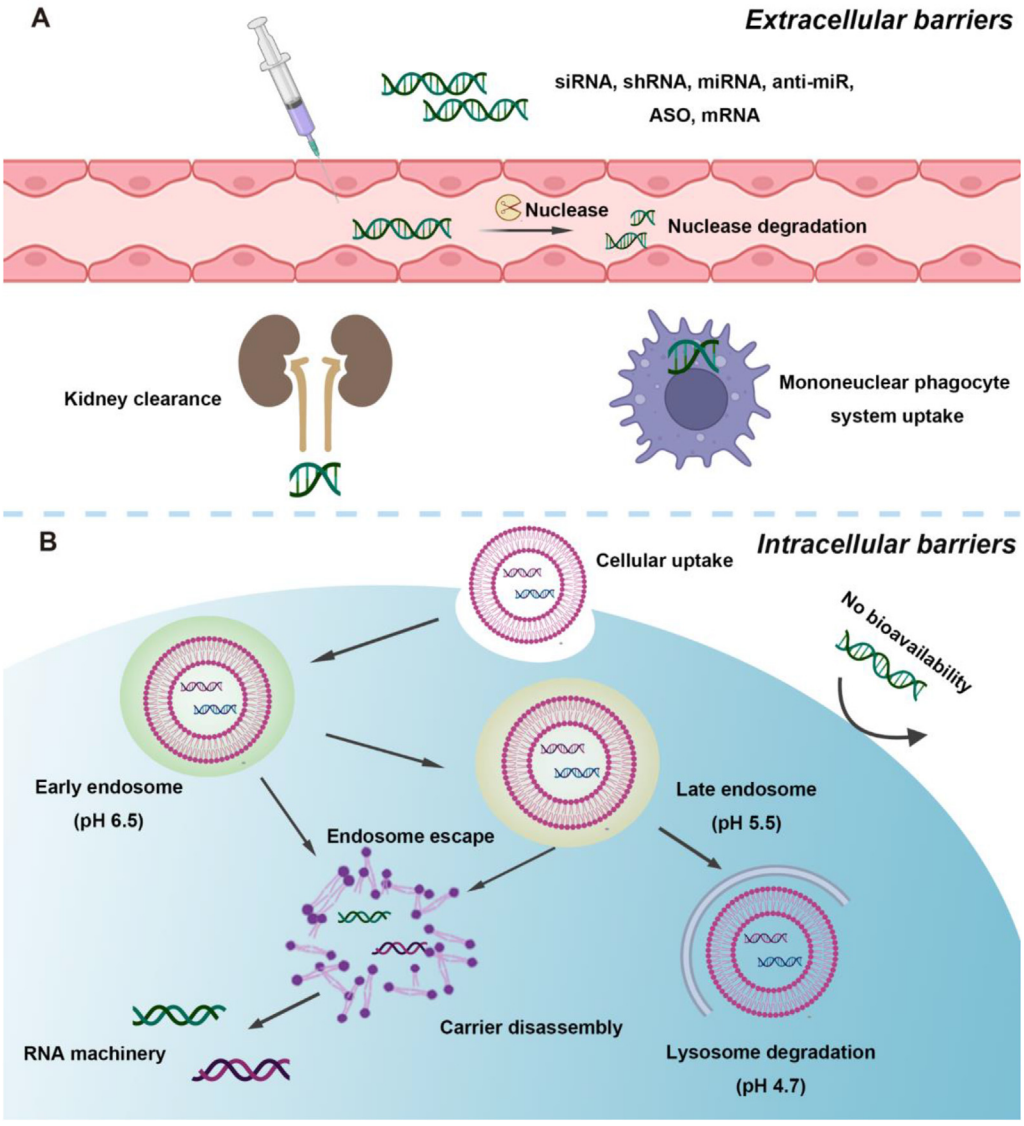

Figure 3 Multiple (A) extracellular and (B) intracellular barriers to RNA delivery following systemic injection.

trimethylammonium propane (DOTMA), 1,2-dioleoyloxy-3-[trimethylammonium]-propane (DOTAP) and *N*,*N*-dioleoyl-*N*, *N*-dimethylammonium chloride (DODAC) (Fig. 4A)[45]. Quaternary ammonium is an organic cation in which a nitrogen atom with a permanently positive charge is covalently bound to four organic substituents. The positive charge at physiological pH enables quaternary ammonium lipids to bind RNAs in aqueous environments strongly. For example, the *in vitro* commercialized gene delivery kit Lipofectin comprises DOTMA and a helper lipid, 1,2-dioleoylphosphatidylethanolamine (DOPE), at a mass ratio of 1:1. However, quaternary ammonium lipids might cause potential cytotoxicity (*e.g.*, hemolysis) and undesirable immunostimulation[46]. One approach to this problem is delocalizing the permanently positive charge on the cationic head groups. Therefore, cationic lipids with head groups of guanidinium, pyridinium, or imidazolium have been developed[47].

4.1.2. Guanidinium lipids

Guanidine is a basic functional group with an acid dissociation constant (pKa) value of approximately 13.5. Hence, guanidine can be protonated throughout an extensive pH range and is permanently positively charged at physiological pH. Arginine, a natural amino acid containing a guanidinium group, was the starting material to synthesize guanidinium-containing cationic lipids. In 2006, Santel et al.[48] synthesized a guanidinium lipid L-arginyl-2-amino-*N*-hexadecyl-*N*-(9*Z*)-9-octadecenyl (AtuFECT01) derived from arginine (Fig. 4A). The lipoplex formulation Atu027 comprising AtuFECT01, commercially available 1,2-distearoyl-*sn*-glycero-3-phosphoethanolamine (DSPE-PEG) and helper lipids DPhyPE was thus developed. Atu027 encapsulating siRNA markedly inhibited protein kinase N3 activity in the endothelium, indicating its use as an effective therapy for pancreatic and prostate cancers in mice[49,50], leading to its evaluation in clinical trials[51].

The multivalent forms of guanidinium lipids produced by coupling guanidine groups with other moieties, such as amines, show more productive transfection activity and less cytotoxicity than its monovalent analogs[52]. For example, Chen et al.[53] developed a series of guanidinium lipids whose head groups were composed of an L-lysine residue and a guanidinium group, such as *N*,*N*-distearyl-*N*-methyl-*N*-2 [*N*′-(*N*2-guanidino-L-lysinyl)] aminoethyl

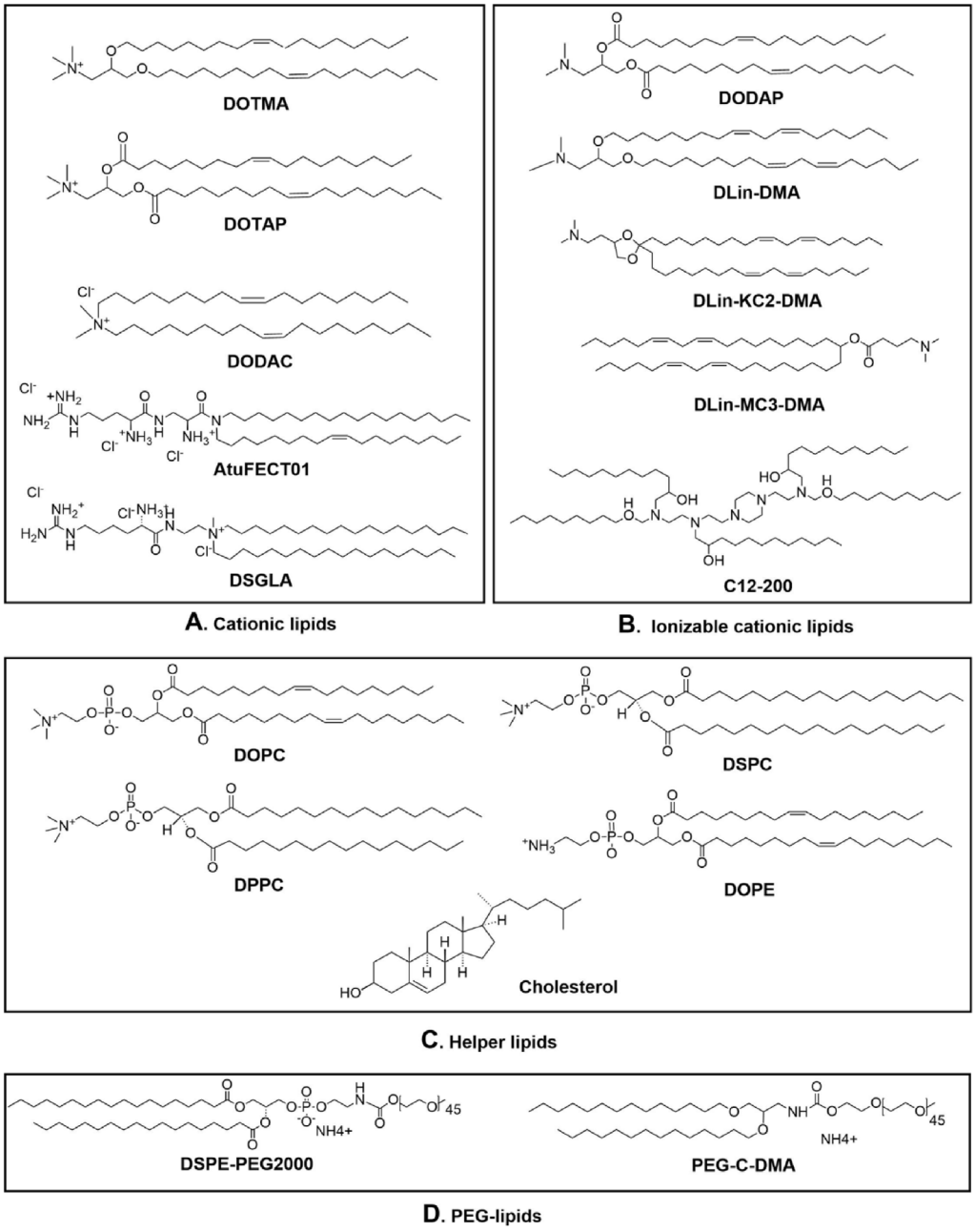

Figure 4 Representative key lipid components used for lipid nanovehicle construction. (A) Cationic lipids, (B) ionizable cationic lipids, (C) helper lipids, and (D) PEG-lipids.

ammonium chloride (DSGLA) (Fig. 4A). SiRNA encapsulated by DSGLA-containing lipopolyplexes downregulated pERK protein expression in H460 cells more effectively than their DOTAP-containing counterpart.

4.1.3. Pyridinium and imidazolium lipids

In addition to guanidinium head groups, the permanently positive charge can be delocalized by introducing heterocyclic rings, *e.g.*, pyridinium and imidazolium rings. Liu et al.[54] developed a series of cyclen-derived cationic lipids containing an imidazole head group. The hydrophilic head group of cyclen carries four amine groups with distinct pK_a values (pK_a = 0.8, 1.6, 9.49, and 10.51). The most basic amines (pK_a = 9.49 and 10.51) were highly protonated at physiological pH, producing good cationic properties. However, the other two amines exhibited too little basicity to be protonated in acidic endosomes (at pH 5.0−6.5). Therefore, adding imidazole with a pK_a value of approximately 6 led to the protonation of the cyclens in the acidic endosomal environment, which promoted their endosomal escape.

4.2. Ionizable cationic lipids

Many ionizable cationic lipids bearing ionizable amino head groups have been synthesized to overcome the limitations of cationic lipids for RNA delivery. Ionizable lipids commonly have a pK_a value < 7 and are thus neutral under physiological

conditions (pH 7.4) and protonated at an acidic pH (pH < 6.0). The lipid nanovehicles formed by ionizable lipids have an overall neutral surface charge and thus exhibit lower toxicity and longer circulation times than cationic lipid-containing counterpart[12]. Furthermore, in acidified endosomes, ionizable lipids become positively charged *via* protonation and thus interact with negatively charged endosomal membranes, causing membrane destabilization and RNA release into the cytosol[55].

3-(Dimethylamino)propane-1,2-diyl dioleate (DODAP) was the first ionizable amino lipid employed in an SNALP formulation (Fig. 4B). In 2001, Semple et al.[11] revealed that ionizable lipid DODAP-loaded SNALPs showed a half-life of 5−6 h. In contrast, their cationic lipid DODAC-containing counterpart showed a shorter half-life of 15 min. This difference was attributed to DODAP having a pK_a value 6.6, leading to low surface charge intensity at physiological pH. Subsequently, Heyes et al.[56] revealed that increasing the number of double bonds in the hydrophobic tails of ionizable lipids (increasing the unsaturation degree) promoted the transition into the fusogenic HII hexagonal phase of the SNALP. DODAP has two oil acyl hydrophobic tails, one of which is a C18 chain with a single cis double bond. Endosomal fusion and delivery efficiency were considerably enhanced when the number of double bonds nearby was increased to 2. The resulting lipid, called 1,2-dilinoleyloxy-3-dimethylaminopropane (DLin-DMA), led to effective RNAi in nonhuman primates for the first time after systemic administration with LNPs, becoming the first ionizable lipid to be entered in a clinical trial (Fig. 4B)[57].

Next, the linker connecting linoleyl chains to the remaining part of the lipid was optimized. A carbon atom in a ketal ring linking both chains led to substantially increased potency. Moreover, the length of the carbon linker between the head group and the remaining lipid structure exerted an apparent effect on pK_a. Furthermore, the spacer of two carbon atoms showed superior potency. Therefore, 2,2-dilinoleyl-4-dimethylaminoethyl-1,3-dioxolane (DLin-KC2-DMA) with a ketal ring and two carbon spacers was identified as the best-performing lipid by screening (Fig. 4B)[58]. Then, the structure of DLin-KC2-DMA was optimized. Jayaraman et al.[59] found that replacing the ketal ring with a carboxylic ester but maintaining the single carbon bond of KC2 to the linoleyl chains led to higher RNAi efficacy. The lipid (6*Z*,9*Z*,28*Z*,31*Z*)-heptatriacont-6,9,28,31-tetraene-19-yl 4-(dimethylamino) butanoate (DLin-MC3-DMA) was identified by screening and used in the Onpattro product (Fig. 4B)[60].

Although MC3 is not biodegradable, it is safe when administered at 0.3 mg/kg every three weeks in Onpattro. However, biodegradability may be necessary for lipid formulations that require frequent dosing. For instance, mRNA payloads encode a therapeutic protein. It is an effective strategy to insert carboxylic ester groups into ionizable lipids that can be cleaved by esterases. The degradation time depends on the location of the carboxylic ester moiety. L319 was rapidly degraded *in vivo*, whereas L343 showed prolonged stability, presumably because of steric hindrance preventing the enzyme from reaching the ester. These biodegradable lipids are reported to be more potent than MC3[61].

Other lipids known as lipidoids or lipid-like compounds can be easily synthesized *via* combinational chemistry. A unique advantage of this approach is that numerous lipids can be developed by assembling changeable building modules, which, combined with high-throughput screening, has allowed the rapid discovery of potent ionizable lipids[62,63]. The first lipidoid, 98N12-5, transports siRNA to hepatocytes[63] and endothelial cells[64], but high doses are required. The later generation of lipidoids, such as 1-[2-[bis (2-hydroxydodecyl)amino]ethyl-[2-[4-[2-[bis(2-hydroxydodecyl) amino]ethyl]piperazin-1-yl]ethyl]amino]dodecan-2-ol (C12-200), shows higher potency (Fig. 4B)[62].

4.3. Helper lipids

Helper lipids, such as phosphatidylcholines (PCs), DOPE, and cholesterol, are crucial formulation components that promote formulation stability, membrane fusion, and endosome escape[65].

4.3.1. Phosphatidylcholines

PCs, one of the major components of cell membranes, easily form a bilayer phase due to their cylindrical geometry. 1,2-Dioleoyl-*sn*-glycerol-3-phosphatidylcholine (DOPC) with unsaturated tails has a low phase transition temperature (T_m) and exists in a fluid state at physiological temperature, making the lipid nanovehicles it forms susceptible to serum protein opsonization[66]. Furthermore, DOPC is less effective in transfection than DOPE because it tends to form a stable structure (Fig. 4C)[67]. Indeed, Hattori et al.[68] found that a DOTAP plus DOPC formulation showed transfection rates inferior to those of DOTAP plus DOPE because the DOPC-containing lipoplexes were trapped in late endosomes. In contrast, the DOPE-loaded lipoplexes rapidly escaped from endosomes.

PCs with saturated tails, such as 1,2-distearoyl-*sn*-glycero-3-phosphocholine (DSPC) and 1,2-dipalmitoyl-*sn*-glycero-3-phosphocholine (DPPC), have a relatively high T_m and are commonly used for the preparation of highly stable LNPs (Fig. 4C)[69]. The Cullis group found that in blank LNP systems, DSPC−cholesterol existed in the outer layers of LNPs, whereas DSPC−cholesterol was partially internalized with siRNAs into siRNA-loaded LNPs. By participating in the formation of siRNA-lipid complexes, DSPC increased siRNA encapsulation into LNPs[70]. DSPC is a helper lipid in the marketed LNP products mRNA-1273, patisiran, and BNT162b2.

4.3.2. Dioleoyl phosphatidylethanolamine

DOPE has a relatively small phosphoethanolamine headgroup that binds to two bulky and unsaturated oleoyl chains *via* an ester linker (Fig. 4C). Because of its low T_m (30 °C), DOPE can enter an inverted hexagonal (HII) phase at physiological temperature, which is conducive to membrane fusion and bilayer disruption[68]. Thus, DOPE is commonly described as a fusogenic lipid. However, DOPE-containing vectors have relatively low colloidal stability because of bilayer fusion-induced size increase during storage and enhanced interplay with serum proteins in the circulatory system[71]. Furthermore, excessive fusion leads to undesirable cytotoxicity. DOPE is a primary component of several lipoplex formulations on the market, *e.g.*, lipofectamine (a mixture of 3:1 (*w*/*w*) of *N*-[2-({2,5-bis [(3-aminopropyl)amino]-1-oxopentyl}amino)ethyl]-*N*,*N*-dimethyl-2,3-bis[(1-oxo-9 octadecenyl)oxy] salt with hydrogen chloride (DOSPA) and DOPE) and lipofectin (a mixture of 1:1 (*w*/*w*) of DOTMA and DOPE)[72,73].

4.3.3. Cholesterol

By filling in gaps between phospholipids, cholesterol stabilizes lipid bilayers in the circulatory system (Fig. 4C)[71,74]. For example, incorporating cholesterol into liposomes increased their stable time in the bloodstream from several minutes to over 6 h[75]. In addition, cholesterol promotes interactions between lipoplexes and cellular or endosomal membranes[76]. As a helper lipid in LNP

formulations, cholesterol generally performs better than DOPE despite its lower fusogenic tendency[77]. The presence of cholesterol and PCs leads to the formation of stable bilayers and is frequently used in LNP formulations[78].

4.4. PEG-lipids

PEG-lipids comprise a hydrophilic PEG polymer covalently bound to a hydrophobic lipid anchor; they include DSPE-PEG and *N*-[(methoxy poly (ethylene glycol)2000)carbamoyl]-1,2-dimyristyloxlpropyl-3-amine (PEG-C-DMA) (Fig. 4D). The incorporation of a PEG-lipid into lipid nanovehicles increases colloidal stability *in vitro*. For example, without a PEG-lipid, the ethanolic environment and low pH of the LNP manufacturing process can accelerate particle fusion to induce particle size amplification. Moreover, PEG-lipids in lipid nanovehicles can prevent serum protein opsonization and MPS clearance and thus prolong their circulation time *in vivo*. A longer retention time in the blood means that the particles are more likely to distribute to disease sites, such as solid tumors, *via* the enhanced penetration and retention (EPR) effect.

However, a PEG polymer can form a steric barrier that prevents cellular uptake and endosome escape, decreasing RNA delivery efficiency[79]. Various strategies have been developed to address this dilemma. First, PEG can be adopted at a low mole percentage. For example, Semple et al.[58] revealed that a 5-fold increase in siRNA's *in vivo* delivery efficiency was achieved when the PEG content was decreased from 10% to ∼1.5%. Second, a PEG-lipid with a short hydrophobic tail can be used. For instance, PEG-C-DMA carries a relatively short myristic lipid anchor (14 carbons), not a stearoyl (18 carbons) tail, as in DSPE-PEG. Thus, PEG-C-DMA gradually detaches from the LNP surface in the circulatory system[80]. This detachment of PEG-C-DMA reduces the PEG density, which is conducive to liposome interaction with cellular or endosomal membranes and, thus, better intracellular delivery. Third, PEG-lipids can be covalently decorated with ligands to target cell-specific membrane receptors to increase the cellular uptake of the lipid nanovehicles. Lipopolyplexes bearing DSPE-PEG-anisamide targeted the sigma receptor on B16F10 cells and showed efficient intracellular delivery of siRNA[81].

5. Fabrication methods and corresponding lipid nanovehicles

5.1. Fabrication methods

Various methods, such as simple mixing, thin-film hydration, precomplexation followed by liposomal coating, ethanol dilution, and T-mixing or microfluidics-mixing, have been used for lipid nanovehicle construction. Among these processes, the T-mixing or microfluidics-mixing technique is a scalable production method. Notably, fabrication methods exert crucial effects on lipid-based nanostructures and RNA encapsulation efficiency.

5.1.1. Simple mixing of RNAs with preformed liposomes

The simplest way to prepare lipoplexes is by incubating preformed cationic liposomes with an RNA solution (Fig. 5A). This method is applicable for liposomes with no or low PEG coverage on their surface, facilitating the sandwiching of RNAs between multilayered lipid structures. For instance, complexes were formed by incubating siRNAs with DOTAP−cholesterol liposomes containing liver-targeting ligands[82]. After complexation with siRNA, the liposome was increased from 150−175 nm to 180−200 nm, indicating a multilayer formation. The surface potential declined from 50 mV to 40 mV, indicating that some of the siRNA molecules remained on the external leaflets of the liposomes. SDS-PAGE assays showed that a high percentage of siRNAs was protected from degradation in human serum, suggesting that most of the siRNAs had been encapsulated inside the liposome. In addition, cationic liposomes containing low superficial PEG coverage also formed protective complexes. For example, the size of preformed cationic liposomes comprising AtuFECT01/DPhyPE and 1 mol% DSPE-PEG with an initial size of ∼60 nm was approximately doubled after complexing with siRNAs[48]. However, this method does not apply to liposomes with high PEG densities because RNAs bind only to the external surface of liposomes under such conditions (Fig. 5A).

5.1.2. Surface modification of preformed lipoplexes with PEG (PEGylation)

Although PEGylation prevents the formation of protective lipid multilayers *via* steric hindrance, non-PEGylated cationic liposomes can be easily eliminated by MPS *in vivo*. Decorating PEG chains on the surface of preformed non-PEGylated lipoplexes can effectively prevent their phagocytosis, and these chains can be added by incubating the lipoplexes with a micellar suspension of PEG-lipids at high temperature; this is called the postinsertion method (Fig. 5B)[83]. PEG chains can shield the surface charge of the liposomes. Therefore, PEG-lipid insertion can be confirmed by measuring the zeta potential. Alternatively, PEGylation can be achieved by covalently conjugating PEG chains to preformed lipoplexes, although this technique is only sometimes used[84].

5.1.3. Thin-film hydration method

RNA molecules are negatively charged and thus cannot cross the lipid bilayer of preformed PEGylated cationic liposomes. However, when RNA molecules are complexed within the inner leaflet of liposomes, they are protected from premature liberation or degradation in the blood circulatory system. An easy method to synthesize these complexes involves hydrating a dry, thin lipid film using a concentrated RNA solution, through which approximately one-half of the RNA molecules are encapsulated and located on the liposome inner leaflet (Fig. 5C)[85]. This encapsulation occurred because negatively charged RNA molecules are distributed evenly over all cationic charges in the liposome's inner and outer leaflets.

5.1.4. Precomplexation of RNAs followed by liposome coating

RNA molecules can be complexed with polymers (*e.g.*, protamine and poly (lactic-co-glycolic acid) (PLGA)) or inorganic nanoparticles [*e.g.*, calcium phosphate (CaP) and silicon dioxide (SiO_2)] followed by liposome coating and final PEG grafting (Fig. 5D). Pre-encapsulation of RNA molecules into nanoparticle cores enhances the encapsulation efficiency within liposomes. In addition, CaP cores can be rapidly dissolved in acidic endosomes, induce nanoparticle disassembly, and increase osmotic pressure to induce endosome swelling, thereby promoting RNA release into the cytoplasm[86]. Furthermore, PEGylated liposome coatings protect the nanocores from degradation in the circulatory system[87].

5.1.5. Ethanol dilution method

In addition to the thin-film hydration method, the ethanol dilution method distributes RNA molecules over all cationic charges in a

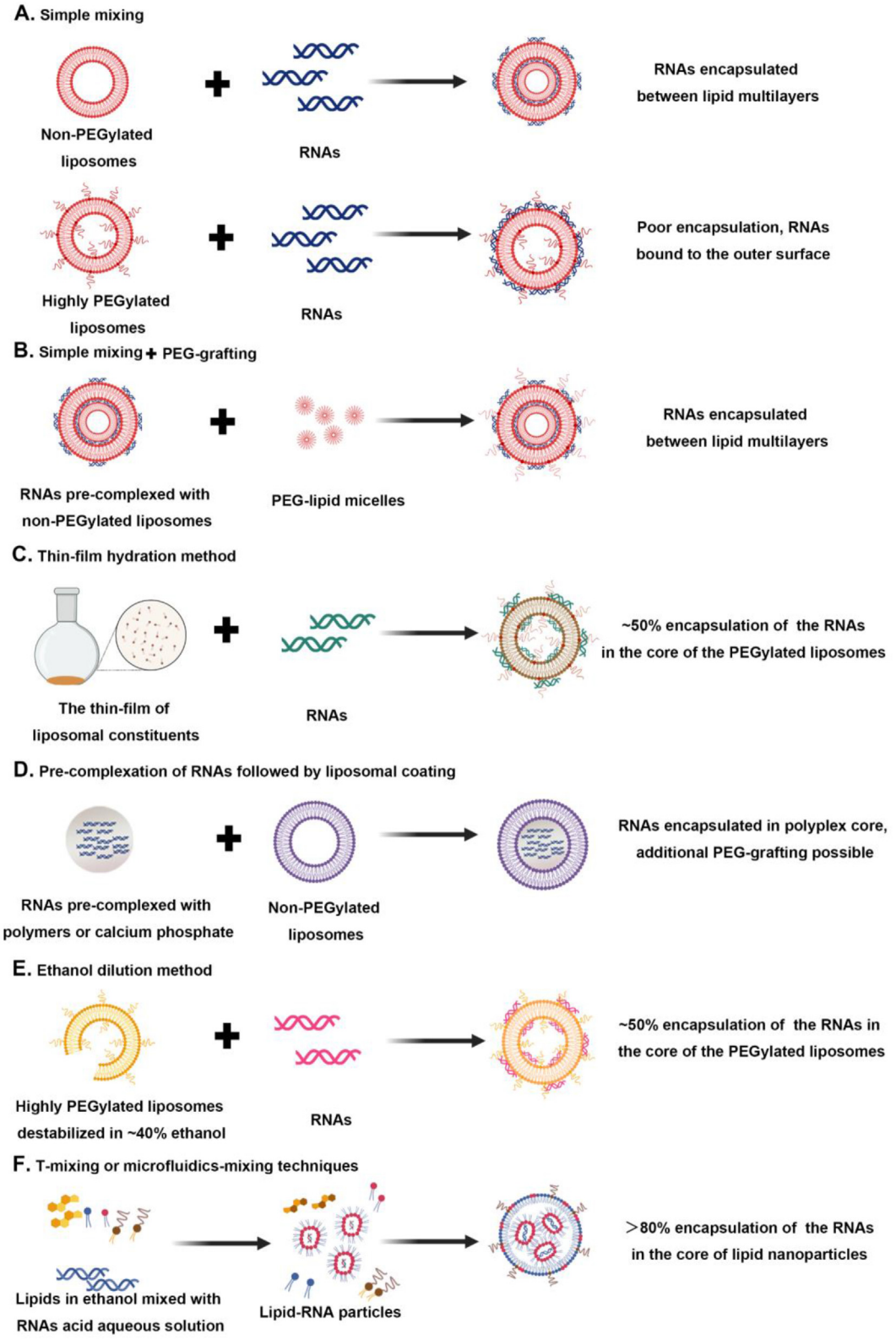

Figure 5 Various methods for lipid nanovehicle fabrication. (A) Simple mixing of preformed cationic liposomes with an RNA solution. (B) Non-PEGylated lipoplexes are decorated with PEG by incubating with a micellar suspension of PEG-lipids at high temperatures. (C) Thin-film hydration method. (D) RNA molecules are precomplexed with polymers or inorganic nanoparticles, followed by liposome coating. (E) Ethanol dilution method. (F) T-mixing or microfluidics-mixing technique.

highly PEGylated cationic liposome (Fig. 5E). Through this approach, PEGylated cationic liposomes and RNAs are mixed in a buffer with a critical concentration of ethanol (~40%), which destabilizes liposomes and allows RNA molecules to penetrate the lipid bilayer. Then, the ethanol is eliminated by tangential filtration or dialysis, leading to the generation of closed PEGylated liposomes. Similar to the direct hydration method, this method induces 50% encapsulation of RNA molecules into liposomes, and the RNAs have been confirmed to be evenly distributed along all cationic charges of the liposomes. Notably, a suitable ethanol concentration must be used when applying this method. An ethanol concentration that is too low results in insufficient liposome destabilization, while an ethanol concentration that is too high induces large-scale liposome aggregation.

5.1.6. *T-mixing or microfluidics-mixing technique*

LNPs are generally prepared by a T-mixing or microfluidics-mixing technique (Fig. 5F). Briefly, an ethanol solution of lipids is mixed with an RNA aqueous solution at an acidic pH using a T-tube or microfluidic mixer. Then, ionizable lipids are protonated and thus form complexes with negatively charged RNAs, as the overall solubility of the lipids is decreased due to ethanol dilution. This complexation leads to the construction of unstable nascent lipid-RNA particles that tend to aggregate until they are diluted in the neutral buffer. This technique applies to many formulation conditions and RNA types and exhibits high RNA encapsulation efficiency (>80%). In contrast to the aqueous compartment surrounded by a lipid bilayer observed in classical liposomes, the formed LNPs have a solid core comprising ionizable cationic lipids and their complexes with RNA payloads, which are coated by a monolayer of structural lipids (*i.e.*, cholesterol, phospholipids) and PEG-lipids[80,88,89]. The technique has been used to produce Onpattro and several other LNPs in the clinical stage of development[60].

5.2. *Corresponding lipid nanovehicles*

A series of lipid nanovehicles can be formed using the above-mentioned fabrication methods. Indeed, based on their physical structures, these nanostructures can be classified into five main types, *i.e.*, lipoplexes, SNALPs, lipopolyplexes, MCNPs, and LNPs. Accordingly, the fabrication methods and critical characteristics of these lipid-based nanostructures are summarized in Table 2.

5.2.1. *Lipoplexes*

Lipoplexes with a diameter of approximately 60−200 nm are commonly fabricated by incubating preformed cationic liposomes with an RNA solution followed by PEG grafting, as indicated in Fig. 5A and B[90]. Lipoplexes generally form multilamellar structures in which RNAs are embedded between adjacent lipid bilayers (Fig. 6A). The typical sandwich structure of lipoplexes can be observed in the cryogenic transmission electron microscopy (Cryo-TEM) images (Fig. 6B)[91]. Several commercially available lipoplex formulations, *e.g.*, Lipofectin, Lipofectamine, and LipoRNAiMAX, are frequently used for *in vitro* gene transfection[92].

5.2.2. *Stabilized nucleic acid-lipid particles*

SNALPs with a particle size of approximately 70−150 nm are constructed by the ethanol dilution method, as shown in Fig. 5E[57,58,93–95]. Only liposomes containing ionizable lipids (*i.e.*, they are cationic at pH 4 and neutral at pH 7.4) can form SNALPs (Fig. 6C). Preformed liposomes are mixed with an RNA solution in acid ethanol-containing complexation buffer (pH 4−5). Due to membrane permeability, RNAs penetrate the liposome interior and adhere to the positively charged internal leaflet *via* electrostatic adsorption. After dialysis against a neutral buffer (pH 7.4), the overall charge on the external surface of these liposomes becomes neutral, causing residual unencapsulated RNAs to detach. The resulting SNALPs exhibit a siRNA encapsulation efficiency higher than 90%. Cryo-TEM images confirmed that SNALPs comprise a hollow core surrounded by a lipid bilayer (Fig. 6D)[96].

5.2.3. *Lipopolyplexes*

Lipopolyplexes are liposomes that enwrap polyplexes (cationic polymer/RNA complexes) (Fig. 6E) and generally have a diameter of approximately 100−200 nm[97]. The concept of lipopolyplexes was derived from plasmid DNA delivery by liposomes[86]. Lipopolyplexes are fabricated by coating a cationic lipid bilayer onto anionic polyplexes or *vice versa* through electrostatic interactions *via* the method shown in Fig. 5D. PEG grafting is commonly required for both *in vitro* and *in vivo* stability[53]. In addition, lipopolyplexes can be prepared by directly hydrating lipid membranes with polyplex dispersions[98]. Shadow area within the cores of lipopolyplexes confirmed the presence of polyplexes as indicated in Cryo-TEM images (Fig. 6F)[98].

5.2.4. *Membrane/core nanoparticles*

MCNPs comprise an inorganic nanoparticle core surrounded by a lipid bilayer shell (Fig. 6G). The cores generally consist of porous CaP or SiO_2 nanoparticles, whose porous surfaces can be loaded with large amounts of RNAs. The bilayer comprises homogenous (symmetric)[87] or mixed (asymmetric) lipids[99]. Symmetric MCNPs are prepared using the method indicated in Fig. 5D, with lipid bilayers coated onto preformed siRNA-loaded nanocores. The fabrication of asymmetric MCNPs is based on a similar procedure, except that the inner and outer layers are coated sequentially. As shown in Fig. 6H, CaP core-containing asymmetric MCNPs showed a clear core-shell structure (Fig. 6H)[99]. The size of MCNPs depends on the size of the nanoparticle core. In some cases, the MCNP size is tiny (~20−30 nm), conducive to tissue penetration and cellular uptake for high RNA delivery efficiency[99]. However, the MCNP synthesis procedure is somewhat complicated because the nanocore and shell must be synthesized.

5.2.5. *Lipid nanoparticles*

LNPs typically consist of ionizable lipids, cholesterol, phospholipids (*e.g.*, PCs), and PEG-lipids. In contrast to traditional liposomes, LNPs form a micellar structure within the internal core, thereby showing more rigid morphology and better kinetic stability than traditional liposomes (Fig. 6I). This supposed structure is supported by the "solid-core" morphology of LNPs as shown in the Cryo-TEM images (Fig. 6J)[12]. Furthermore, LNPs can be prepared *via* fully scalable methods, *e.g.*, a T-mixing or microfluidics-mixing technique (Fig. 5F), leading to homogeneous LNPs with RNA entrapment efficiencies higher than 8%. Indeed, LNPs of specific sizes can be precisely produced by controlling the microfluidic operating parameters, such as the total flow rate and flow rate ratio.

Table 2 Fabrication methods and key characteristics of a series of lipid-based nanostructures used for RNA delivery.

Lipid nanovehicle	Fabrication method	RNA-embedding site	Particle size and surface potential	Advantage and disadvantage
Lipoplexes	Simple mixing of RNAs with preformed cationic liposomes followed by PEG grafting	Between adjacent lipid bilayers	60−200 nm; positive	Disadvantages: Hollow structure leads to weak stability; Fabrication methods using organic solvents are unfavorable for large-scale production
Stable nucleic acid lipid particles (SNALPs)	Ethanol dilution method	Positively charged internal surface of lipid bilayers	70−150 nm; neutral	Disadvantages: Hollow structure leads to weak stability; Fabrication methods using organic solvents are unfavorable for large-scale production
Lipopolyplexes	Precomplexation of RNAs followed by liposome coating and PEG grafting	Polyplex core	100−200 nm; positive or negative	Advantages: Solid nanocore-supported structure has good kinetic stability Disadvantages: Complex fabrication methods are unfavorable for large-scale production
Membrane/core nanoparticles (MCNPs)	Precomplexation of RNAs followed by liposome coating and PEG grafting	Inorganic nanoparticle core	20−60 nm; positive or negative	Advantages: Solid nanocore-supported structure leads to good stability Disadvantages: Complex fabrication methods are unfavorable for large-scale production
Lipid nanoparticles (LNPs)	T-mixing or microfluidics-mixing technique	Micellar core	50−100 nm; neutral	Advantages: Micellar core-supported structure has good stability Facile T-mixing or microfluidic-mixing technique favors large-scale production Homogenous size distribution can be easily obtained by controlling the operational microfluidic parameters

6. Lipid nanovehicle design for overcoming multiple barriers to systemic RNA delivery

As mentioned above, systemic RNA delivery must overcome multiple extracellular and intracellular barriers (Fig. 3). In the blood circulatory system (an extracellular barrier), entrapment by lipid nanovehicles effectively protects RNAs from nuclease degradation and MPS phagocytosis and prevents elimination through the kidneys because the size of the nanovehicles greatly exceeds the pore size of glomeruli (∼8 nm)[36]; however, as foreign particles, nanovehicles can be phagocytized by the MPS, leading to low blood retention and limiting the amount of loaded RNA delivered to target tissues. Therefore, various strategies have been developed to increase the blood pharmacokinetics of lipid nanovehicles; these methods include surface PEGylation, modulation of physicochemical properties, and nanoprimer pretreatment. In addition, to overcome intracellular barriers, the surface properties and formulation constituents of lipid nanovehicles have been extensively tailored to enhance cellular endocytosis and endosome escape.

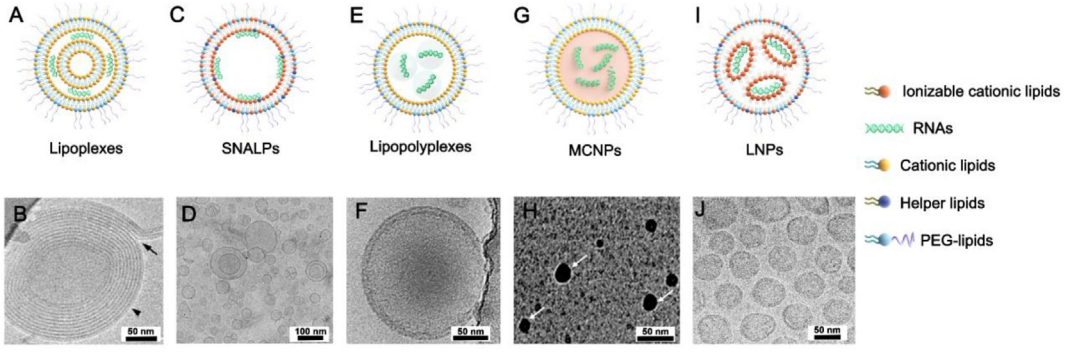

Figure 6 Schematics and the corresponding transmission electron microscopy (TEM) images of lipid nanovehicles used for RNA delivery. (A) Schematic and (B) Cryo-TEM image of lipoplexes. Reprinted with permission from Ref. 91. Copyright © 2004 CELL PRESS. (C) Schematic and (D) Cryo-TEM image of stabilized nucleic acid-lipid particles (SNALPs). Reprinted with permission from Ref. 96. Copyright © 2022 WILEY. (E) Schematic and (F) Cryo-TEM image of lipopolyplexes. Reprinted with permission from Ref. 98. Copyright © 2011 Elsevier). (G) Schematic and (H) TEM image of membrane/core nanoparticles (MCNPs). Reprinted with permission from Ref. 99. Copyright © 2012 Elsevier. (I) Schematic and (J) Cryo-TEM image of lipid nanoparticles (LNPs). Reprinted with permission from Ref. 12. Copyright © 2020 Elsevier.

6.1. *Lipid nanovehicle design for prolonged circulation in the blood*

A prolonged blood circulation time is a favorable property through which liposomes have more opportunities to carry RNAs to target tissues. Liposomes are eliminated mainly *via* postopsonization macrophage phagocytosis in the MPS in the circulatory systems. Through opsonization, plasma proteins are adsorbed to the surface of a foreign nanoparticle. This process thus depends on the properties and components of the nanoparticle formulation. Therefore, nanoproperties of lipid nanovehicles have been optimized for prolonged blood retention. In addition, by occupying the MPS in advance, nanoprimers improve the blood pharmacokinetics of subsequently administered nanovehicles.

6.1.1. *PEGylation*

Surface decoration of lipid nanovehicles with PEG forms a hydrated layer to prevent lipid nanovehicles from aggregation, opsonization, and phagocytosis *via* steric hindrance, leading to prolonged retention in blood. In particular, the modification density of PEG exerts a crucial effect on nanovehicle function. A high PEG density (>8 mol%) destroys the structure of liposomal vesicles, inducing the liposome-to-micelle transition[100]. However, at low surface PEG density (<4 mol%), PEG chains form a 'mushroom' configuration with gaps in the PEG protective layer, and opsonin proteins can freely move through these gaps to bind the liposome surface[101,102]. Therefore, only when the PEG density ranges from 5 to 7 mol% can PEG chains exhibit the "brush" configuration that effectively covers the liposome surface[101].

Although PEGylation is conducive to prolonged blood circulation, PEG polymer forms a steric barrier that prevents cellular uptake and endosome escape of nanovehicles. Phenomena are commonly known as the "PEG dilemma"[79]. Various strategies have been proposed to resolve this problem. First, PEG-C-DMA with short myristyl (14 carbons) hydrophobic tails, compared to stearoyl (18 carbons) anchor for DSPE-PEG, gradually detaches from the LNP surface in the circulatory system to reduce PEG density, facilitating the subsequent interaction of the LNPs with cell and endosome membranes. SNALP formulated with DLin-KC2-DMA, cholesterol, DPPC, and PEG-C-DMA (57.1/7.1/34.3/1.4, *mol/mol/mol/mol*) showed *in vivo* activity at a low siRNA dose (0.01 mg/kg) in nonhuman primates[58]. Second, modification of liposomes with a stimulus-responsive detachable PEG shell is also helpful. Methoxy-$PEG_{5\ k}$-polymethacryloyl sulfadimethoxine ($mPEG_{5\ k}$-SDM_8) can be responsively released from the liposome surface at pH 6.5, which mimics the tumor microenvironment[103]. Accordingly, detachment of the PEG shell exposes the cell-penetrating peptide, which is conducive to intracellular delivery of encapsulated RNA or small-molecule drugs.

Notably, PEGylated lipid nanovehicles bind immunoglobulins (Igs) on reactive B cells in the marginal zones of the spleen, thereby stimulating the secretion of anti-PEG IgM. Accordingly, once a second dose is administered, the previously produced anti-PEG IgM adheres to PEG on nanovehicles, and the complement system is activated, leading to increased phagocytosis by macrophage cells[104–106]. This undesired immunogenic reaction to PEG is commonly known as the "accelerated blood clearance (ABC) phenomenon," which increases the clearance of PEGylated nanovehicles *in vivo*. PEG-lipids with short hydrophobic tails, *e.g.*, PEG-C-DMA, can dissociate rapidly from the lipid bilayer, reducing the occurrence of the ABC phenomenon[58].

6.1.2. *Optimizing the physicochemical properties of nanovehicles*

Particle size exerts essential effects on the long-circulating properties of nanovehicles. First, the nanovehicles must be large enough to prevent renal filtration. Generally, nanovehicles smaller than 10 nm tend to be eliminated from the body *via* renal excretion[107]. Second, the size of the nanovehicles must be small enough to reduce opsonization and MPS clearance. For larger nanovehicles (>200 nm), a low radius of curvature contributes to the adsorption of opsonins and protein assembly into bulkier complexes[108,109]. Therefore, a spherical nanovehicle with a particle size ranging from 10 to 200 nm is optimal[110].

Surface charges are also crucial in determining the *in vivo* fate of nanovehicles. Negative or positive surface charges of nanovehicles promote complement activation and adsorption of plasma proteins and thus accelerate macrophage phagocytosis and clearance from the circulatory system[111]. Hence, neutral nanovehicles generally circulate in blood longer than charged nanovehicles. SNALPs formulated with DODAC (a cationic lipid) and either PEG-CerC14 or PEG-CerC20 showed significantly shorter half-lives (∼15 min and 2−3 h, respectively) than SNALPs formulated with DODAP (an ionizable lipid) and either PEG-CerC14 or PEG-CerC20 (∼5−6 h and 10−12 h, respectively)[11]. These results were attributed to the neutral charge of the ionizable lipids at physiological pH.

The elastic modulus of liposomes also dramatically influences their retention in the blood circulatory system[112]. A higher elastic modulus indicates less compressible interfaces that resist opsonization and is conducive to prolonged circulation. The addition of cholesterol markedly increases the elastic modulus of a lipid bilayer. For example, the elastic area dilation modulus (K_A) values of SOPC and SOPC: cholesterol (1/1, *mol/mol*) are ∼200 and 1200 mN/m, respectively[113]. Similarly, sphingomyelin: cholesterol (1/1, *mol/mol*) bilayers are essentially incompressible (K_A = 1800 mN/m) and are retained in the bloodstream for a prolonged time, laying the foundation for the development of a vincristine liposome[114]. Therefore, cholesterol, which is extensively used as a helper lipid in lipid nanovehicles, contributes to their retention in blood.

6.1.3. *Nanoprimer pretreatment*

Kupffer cells in the liver occupy 80%−90% of the overall macrophage population in the MPS of the body[6,111]. In particular, liver sinusoidal endothelial cells (LSECs) and Kupffer cells take up a large proportion of nanoparticles after systemic administration, decreasing their circulation time. To reduce nanovehicle capture, Saunders et al.[115] designed a liposome with a highly negative surface charge (−99.4 mV) and large size (259 nm). After intravenous injection, liposomes with these unique physicochemical properties transiently occupied the MPS and thus decreased the uptake of siRNA-loaded LNPs by Kupffer cells and LSECs, prolonging their retention in blood. Ultimately, through the action of a nanoprimer, LNPs carrying human erythropoietin (hEPO) mRNA or factor VII (FVII) siRNA increased hEPO production (by 32%) or enhanced FVII silencing (by 49%).

6.2. *Lipid nanovehicle design for enhanced cell internalization*

RNAs take effect within target cells; however, as negatively charged macromolecules, they cannot cross cell membranes and depend on vehicles to enter cells. Hence, nanoproperties of lipid

nanovehicles have been extensively tailored for increased cell internalization of RNAs.

6.2.1. *Ligand functionalization*

Ligand decoration is commonly utilized to promote the cellular uptake of lipid nanovehicles *via* ligand-receptor interactions[116]. Ligands, such as monoclonal antibodies, antibody fragments, proteins, peptides, carbohydrates, glycoproteins, and vitamins, must couple the nanovehicle surface to target cells overexpressing particular surface receptors. Among all the parameters, the specificity of the cell surface receptors and targeting ligands influence cellular uptake efficiency.

The ideal receptors should be highly expressed on target cells and at negligible or low levels on normal tissues or cells. For instance, asialoglycoprotein receptors, exclusively expressed on the hepatocyte surface, bind and internalize β-D-galactose ligands[117]. Therefore, galactose-modified lipoplexes loaded with plasmid DNA generated one order of magnitude higher gene expression in the liver than was generated by unmodified lipoplexes[118]. In another study, after systemic injection, galactose-decorated lipoplexes loaded with siRNA led to a 1.9-fold higher siRNA distribution in liver parenchymal cells than was realized with galactose-free lipoplexes[119]. Similarly, human epidermal growth factor receptor 2 (HER2) in breast cancer, folate receptor in ovarian cancer, and $\alpha4\beta1$ in multiple myeloma have been excellent targets on tumor cells, resulting in considerable success in preclinical studies[116].

Antibodies or antibody fragments show higher affinity and specificity for target receptors than other ligands. Compared with whole antibodies, frequently used in the early days of research, antibody fragments possess lower immunogenicity and superior pharmacokinetic properties and thus are preferred for clinical use[120]. Peptides and peptidomimetics are preferred targeting ligands owing to their easy generation, low cost, and increased resistance to enzymatic cleavage[121]. In particular, many peptides and peptidomimetics with high targeting activity can be identified by screening *via* phage display technology[122]. Cyclic RGD-modified lipoplexes effectively delivered anti-signal transducer and activator of transcription 3 (STAT3) siRNA into melanoma cells *via* integrin receptor-mediated endocytosis, leading to a 2.1-fold increase in cell apoptosis compared to that induced by unmodified lipoplexes[123]. Yang et al.[124] modified lipoplexes with dual peptides specifically targeted to low-density lipoprotein receptor (Angiopep-2) or neuropilin-1 receptor (tLyP-1) and showed higher uptake into glioma cells *via* specific receptor-mediated endocytosis than nonmodified and single-peptide-modified lipoplexes. Ultimately, lipoplexes enhanced the gene silencing and antiproliferation activity of the loaded vascular endothelial growth factor (VEGF) siRNA and docetaxel, producing synergistic antitumor efficacy. In addition, several other types of ligands, *e.g.*, sugars, proteins, and vitamins, have been employed in lipid nanovehicle functionalization for targeted cellular internalization[116].

However, ligand modification has not always translated into positive outcomes. For example, Goren et al.[125] found that liposomes functionalized with a monoclonal antibody (N-12A5) against the erbB-2 oncoprotein showed no efficacy against breast cancer cells owing to their inefficient internalization. In addition, Gabizon et al.[126] reported that modification with folic acid promoted liver uptake of liposomes, thereby accelerating their clearance from circulation. These results were attributed to changes to the surface properties of lipid nanovehicles caused by ligand modification, and these changes stimulated the adsorption of plasma proteins to generate a protein corona. The protein corona not only accelerated nanovehicle elimination from the circulatory system by intensifying macrophage uptake but also compromised the targeting ability by shielding ligands. An effective strategy to resolve this dilemma is the reversible shielding of targeting ligands using linkers that can be cleaved in response to extracellular stimulus, *e.g.*, an acidic microenvironment or a tumor-associated enzyme[7,9,127,128]. Overall, the influence of ligand decoration on the *in vivo* fate of lipid nanovehicles still needs to be carefully evaluated.

6.2.2. *Cell membrane fusion functionalization*

Fusogenic lipid nanovehicles do not require receptor-mediated endocytosis and directly introduce RNAs into the cytoplasm, leading to enhanced cellular internalization. For example, Kim et al.[129] developed a fusogenic MCNP comprising a porous silicon nanocore and an external sheath of homing peptides. Through the guidance of the peptide ligands, the MCNPs specifically target macrophages and release their siRNA payload into the cytoplasm *via* membrane fusion. Efficient silencing of IRF5, a proinflammatory marker, increased the clearance ability of macrophages, thereby prolonging the survival of mice with *Staphylococcus aureus* pneumonia. Furthermore, researchers discovered that the fusogenic feature of MCNPs was due to the specific proportions of structural lipid (DMPC), cationic lipid (DOTAP), and PEG-lipid (DSPE-PEG) components[130]. DMPC was the main structural component, and its phase transition temperature (24 °C) was lower than the body temperature (37 °C). This property enabled the lipids to undergo a fluidic liquid−crystal phase transition, facilitating MCNP fusion with cell membranes. In addition, the positive charge of DOTAP promoted uptake and fusion owing to the electrostatic attraction between the MCNPs and the anionic plasma membrane. Ultimately, the PEG-lipid DSPE-PEG can dehydrate the gaps between the fusogenic MCNP lipid bilayer and the plasma membrane, making lipid fusion structurally and energetically favorable.

6.2.3. *Biomimetic modification*

Biomimetic camouflage strategies leverage the inherent ability of cells to interact with their environment, bestowing traditional nanoparticles with cell-targeting function[131]. For example, a previous study reported that adhesion molecules with homotypic adhesion domains on the cancer cell membrane, *e.g.*, *N*-cadherin, galectin-3, or epithelial cell adhesion molecule, facilitated multicellular aggregation formation. Thus, coating with cancer cell membrane endows the lipid nanovehicles with homotypic targeting capability by completely replicating cell surface antigens[132]. For example, Liu et al.[133] constructed azidosugar-loaded pH-sensitive liposomes fused with cancer cell membranes for tumor cell-specific glycan engineering. Notably, through multiple membrane receptors, membrane-camouflaged liposomes showed higher glycan-labeling efficiency than single-ligand-modified liposomes. This homotypic targeting strategy can also enhance cell internalization of RNA molecules.

6.3. *Lipid nanovehicle design for promoting endosomal escape*

Except for lipid nanovehicles with cell membrane-fusing capability, lipid nanovehicles are generally delivered into early endosomes, which then fuse with late endosomes and lysosomes. Sahay et al.[134] reported that approximately 70% of internalized siRNA cargoes underwent exocytosis *via* LNP efflux out of late endosomes/lysosomes, mediated by a lysosomal surface protein of Niemann Pick type C1. The remainder of the endocytosed siRNA

undergoes lysosomal degradation or enters other nonproductive pathways. By directly monitoring gold nanoparticles covalently modified to siRNAs, Gilleron et al.[135] found that endosomal escape of siRNAs was rare (<2%) and occurred in a narrow time window when the LNPs were located in early and late endosomes. In contrast, a higher percentage of mRNAs than siRNAs have been reported to be released from endosomes, with some studies reporting 15%, which depended on ionizable lipid fusogenicity[61,136]. These results demonstrate that endosomal escape is a crucial efficiency-limiting factor for successful RNA delivery. Various strategies have been developed for increasing the endosomal escape efficiency of lipid nanovehicles, and they are described in the following subsections.

6.3.1. *Endosomal membrane destabilization and pore formation*

The most commonly proposed factors destabilizing endosomal membranes are cationic charge and membrane-destabilizing peptides. Moreover, persistent membrane destabilization induces pore formation, allowing smaller particles or molecules to leak from endosomes into the cytoplasm.

Since the external leaflet of endosomal membranes comprises negatively charged phospholipids, the interplay of intraluminal lipoplexes with the endosomal membrane is thought to cause anionic phospholipids to flip from the cytosolic side to the intraluminal side of an endosome[137,138]. The charge-neutralized ion pair leads to a nonlamellar phase transition, destabilizing the membrane. Cationic lipids with quaternary amine groups can confer a permanent positive charge, such as DOTMA and DOTAP. Alternatively, ionizable lipids, including DODAP and DLin-DMA, can endow liposome membranes with a cationic charge in acidified endosomes, and this type of membrane destabilization occurs mainly in acid endosomes. In addition, some amphiphilic peptides with lysine residues (*e.g.*, KALA (WEAKLAKALAKALAKHL AKALAKALKA) and K5) and cell-penetrating peptides (CPPs) (*e.g.*, TAT and other arginine-rich CPPs) can cause membrane destabilization *via* cationic interplay with the endosome membrane[139]. Miura et al.[140] reported a KALA-modified lipopolyplex that allowed the pDNA payload to be efficiently released into the cytoplasm in marrow-derived dendritic cells. Ultimately, the KALA-modified lipopolyplex showed transfection activity ~ two orders of magnitude higher than its R8-modified counterpart.

6.3.2. *Endosomal membrane rupture*

Li et al.[87,99] developed an MCNP comprising a CaP core coated with a lipid bilayer for siRNA delivery. They suggested that *via* the CaP material was dissolved in acidic endosomes after entering the cells *via* endocytosis, leading to liposome disintegration[93]. Then, the released calcium and phosphate ions enhanced the osmotic pressure, leading to endosome swelling and bursting. Accordingly, siRNA molecules, calcium ions, and phosphate ions were released into the cytosol. Notably, sufficient CaP must be transported to the same endosome simultaneously for osmotic pressure-induced membrane rupture, which is often tricky under *in vivo* conditions[99].

6.3.3. *Endosomal membrane fusion*

Fusion with the endosomal membrane promotes lipid nanovehicles to release payloads into the cytosol, and fusion is mediated mainly by fusogenic lipids and cationic lipids. When reaching an endosome, cationic lipids interact with the negatively charged endosomal membrane *via* electrostatic interactions, causing membrane destabilization. Then, after acidification, fusogenic helper lipids such as DOPE transform a lipid nanovehicle in the liquid phase into an inverted hexagonal configuration, thereby facilitating its insertion into the endosomal membrane and enabling fusion[141]. In addition, cholesterol has been added to lipid nanovehicles to promote fusion in a pH-independent manner[76]. Starting with DLin-DMA, Semple et al.[58] used the pK_a and bilayer-to-hexagonal H_{II} transition temperature ($T_{BH,}$ an indicator of membrane fusion activity) parameters to guide the design of an ionizable cationic lipid with superior delivery ability. The best-performing lipid was DLin-KC2-DMA, formulated with DSPC/cholesterol/PEG lipid into an SNALP. The SNALP showed *in vivo* activity at siRNA doses of as low as 0.1 mg/kg in nonhuman primates and 0.01 mg/kg in rodents.

7. Lipid nanovehicle-based RNA drugs on the market and in the clinical trial stage

Three lipid nanovehicle-based RNA therapeutics have been approved for clinical application, including Alnylam patisiran, Pfizer BNT162b2, and Moderna mRNA-1273. Patisiran is an siRNA drug used for treating transthyretin-induced amyloidosis, while the other two drugs are mRNA vaccines for preventing COVID-19. Patisiran is the first nonviral delivery vector approved by the U.S. Food and Drug Administration (FDA) for RNA delivery, marking the initiation of nucleic acid nanomedicine.

Among all three FDA-approved products, only patisiran is administered by systemic injection, which was thus emphatically introduced. In addition to siRNA molecules, the specific components of patisiran include DLin-MC3-DMA (an ionizable cationic lipid), DSPC (a helper lipid), cholesterol (a helper lipid) and PEG-C-DMG (a PEG-lipid)[60]. DLin-MC3-DMA with a pK_a value of 6.2−6.5 exhibited a positive charge at pH 4, facilitating the encapsulation of negatively charged siRNAs. As mentioned above, by taking part in the formation of siRNA-lipid complexes, DSPC plus cholesterol increased siRNA encapsulation efficiency into LNPs[70]. Then, when the medium pH was converted to the physiological value (pH 7.4), the surface charge of the LNPs was neutral. The inclusion of cholesterol enhanced LNP stability in the circulatory system[142]. The introduction of PEG-C-DMG prolonged the blood retention of patisiran. Moreover, PEG-C-DMG with short acyl chains (C14) gradually dissociated from the LNP surface, inducing endogenous apolipoprotein E (ApoE) adsorption[143]. After accumulating in the liver, ApoE promoted hepatocyte LNP uptake *via* ApoE receptor-mediated endocytosis. Then, in acidic endosomes, DLin-MC3-DMA was protonated and thus destabilized the endosomal membrane, and when combined with the membrane-fusing action of cholesterol, these LNPs escaped from endosomes. Accordingly, the released siRNA inhibited hereditary transthyretin amyloidosis (hATTR) mRNA expression in the cytoplasm, downregulating the TTR protein misfolding rate[60]. A study with rats using a ^{14}C-labeled ionizable lipid (^{14}C-MC3) reported that approximately 90% of the radioactive lipid that had been injected was detected in the liver at 4 h after systemic injection with a single dose of patisiran, indicating the excellent liver targeting of these LNPs[144].

The list of lipid nanovehicle-based RNA drugs in the clinical trial stage includes siRNAs, mRNAs, miRNAs, ASOs, and so on (Table 3). Among these lipid nanovehicles, LNPs have been the most extensively used (21/26) because of their unique clinical advantages. As mentioned above, LNPs contain a micellar internal core and exhibit a rigid morphology, resulting in higher kinetic stability. Moreover, they can be controllably prepared *via* a large-scale method, such as T-mixing or microfluidics-mixing

technique, showing RNA encapsulation efficiencies higher than 80%

8. Challenges

As shown in Table 3, numerous lipid nanovehicle-based RNA drugs are being evaluated in clinical trials, confirming the great potential of lipid nanovehicles for RNA delivery. However, only three LNP-based RNA drugs, including Alnylam patisiran, Moderna mRNA-1273, and Pfizer BNT162b2, have been approved by the FDA for clinical use. The data reveal that the clinical transformation of lipid nanovehicles is hindered by significant challenges, especially those related to biosafety and targeting beyond the liver.

8.1. *Biosafety*

Safety is paramount compared to the potency of lipid nanovehicles, and it is the deciding factor for the courses of drug and drug delivery system development, clinical translation, and ultimate success. Lipid nanovehicle- or RNA payload-induced cytotoxicity, immunotoxicity, or immunogenicity severely hinders clinical application.

8.1.1. *Cytotoxicity*

Under some circumstances, cationic lipids cause cytotoxicity by inhibiting cell mitosis, forming vacuoles in the cytoplasm, or damaging crucial cellular proteins, *e.g.*, protein kinase C[146]. The hydrophilic head groups of cationic lipids exert important effects on their cytotoxicity. For example, quaternary ammonium head group-bearing cationic lipids are more toxic than those with tertiary amine head groups[145].

8.1.2. *Immunotoxicity*

RNAs, such as siRNAs and mRNAs, can activate the innate immune system and stimulate the secretion of cytokines *in vivo* and *in vitro*[146,147]. The potentially deleterious results of these responses are exemplified by mice treated with immunostimulatory siRNAs that showed signs of toxicity, including elevated levels of serum alanine and aspartate aminotransferases and reduced numbers of lymphocytes and platelets[148,149]. Notably, RNAs' sequence and chemical nature dictate their gene regulation efficiency and ability to stimulate immune responses[147]. Accordingly, intense interest is focused on identifying chemical modifications that can preserve RNA modulation efficacy while not stimulating immune responses. A 2′-*O*-methyl decoration has been shown to attenuate the immunostimulatory effects of siRNA greatly[150]. MRNA modified with *N* (1)-methylpseudouridine (m1Ψ) alone or in combination with 5-methylcytidine (m5C) induced significantly higher reporter gene expression than pseudouridine (Ψ) or m5C/Ψ-decorated mRNA[151]. Furthermore, m5C/m1Ψ-modified mRNA induced lower intracellular innate immunogenicity than m5C/Ψ-modified RNA after *in vitro* transfection, enhancing cell *via*bility[151]. Nevertheless, administering RNA over a certain dose threshold *via* LNP format still risks immune activation and induces cytotoxicity.

Compared to RNAs, ionizable lipids lead to higher immunotoxicity. Abrams et al.[152] found that systemic injection of LNPs bearing ionizable lipids of 2-{4-[(3*b*)-cholest-5-*en*-3-yloxy]-butoxy}-*N*,*N*-dimethyl-3-[(9*Z*,12*Z*)-octadeca-9,12-dien-1-yloxy]-propan-1-amine (Clin-DMA) stimulated the production of pro- and anti-inflammatory cytokines, which was primarily attributed to their lipid components and, to a lesser extent, their payloads. In addition, systemic administration of LNPs can induce serum complement activation, ultimately leading to non-IgE-mediated hypersensitivity reactions (HSRs)[152−155]. Moreover, complement activation-related HSRs are unpredictable and occasionally lead to lethal outcomes[154].

Interventions have been implemented to attenuate the immunotoxicity associated with lipid nanovehicles and expand the therapeutic window; these interventions include premedication or codelivery with corticosteroids (*e.g.*, dexamethasone), the application of pathway-specific inhibitors (*e.g.*, Janus kinase inhibitor), and the use of reinforced PEG shielding. By activating glucocorticoid receptors in multiple cell types, immunosuppressive drugs such as dexamethasone attenuated the generation of several proinflammatory factors[156]. In 2010, Abrams et al.[152] showed that after mice were intraperitoneally injected with increasing doses of dexamethasone 1 h prior to LNP dosing, the levels of at least six cytokines were reduced to near basal levels. For this reason, corticosteroid premedication has extensively been employed in the clinical[157]. However, chronic steroid medication may lead to undesired side effects.

By regulating the receptors for several cytokines associated with inflammatory responses, the Janus kinase-signal transducer and activator of transcription (JAK-STAT) pathway plays a crucial role in immune modulation[158]. Tao et al.[159] reported that inhibiting the JAK-STAT pathway reduced the immune stimulation induced by LNPs. Pretreatment with 2 doses of a JAK inhibitor before systemic injection of LNPs attenuated LNP-induced lethality in rats, and this outcome was accompanied by significant mitigation of all relevant toxicity-induced responses. Furthermore, this medication may be superior to corticosteroids, which induce multiple immunosuppressive side effects.

PEG shielding has been another practical approach to attenuating lipid nanovehicle interplay with serum proteins and complements. Kumar et al.[155] reported that increasing the amount of PEG grafted from 1.5% to 10% (*mol*/*mol*) decreased cytokine secretion, complement activation, and LNP recognition by macrophages in a murine model. However, as expected, high PEG coverage suppressed LNP uptake by target cells, reducing their gene-silencing efficacy. Therefore, optimizing the PEG molar ratio for maximum protection of LNPs from the immune system is crucial without compromising their effectiveness.

8.1.3. *Immunogenicity*

As mentioned above, PEGylated lipid nanovehicles can stimulate B cells in the spleen to generate anti-PEG IgM antibodies, thereby exacerbating the clearance of a second dose of PEGylated nanovehicles (the ABC phenomenon)[104−106]. IgM, a well-known opsonin, can recognize foreign bodies and trigger complement activation, eventually leading to phagocytosis[160]. Judge et al.[161] reported that "diffusible" PEG lipids rapidly dissociating from the lipid nanovehicle surface ameliorated PEG-induced antibody responses. They prepared various PEGylated liposomes harboring PEG lipids with different lengths of alkyl chains (C14, C16, and C18). They found that the PEG lipids with a short alkyl chain (a C14 chain) caused a 10-fold reduction in anti-PEG antibodies at 7 days after intravenous injection in mice compared to the effect of PEG lipids with a long alkyl chain (a C16 or C18 chain). In addition, by injecting liposomes in 2-week intervals or with washout periods between the injections, the ABC effect was largely attenuated, presumably due to the short biological half-life of IgM. Notably, these studies were conducted with animal

Table 3 Representative clinical trials evaluating lipid nanovehicle-based RNA therapeutics.

Therapeutic modality	Name	Disease	Target	Delivery system	Delivery route	Phase	Start year	Status	Clinical trial identifier
siRNA	PRO-040201	Hypercholesterolemia	ApoB	LNP	IV	I	2009	Terminated	NCT00927459
	TKM-080301	ACC and NET	PLK1	LNP	IV	I/II	2010	Completed	NCT01262235
	ALN-PCS02	Hypercholesterolemia	PCSK9	LNP	IV	I	2011	Completed	NCT01437059
	TKM-100201	Ebola virus infection	VP24, VP35, L-polymerase	LNP	IV	I	2012	Terminated	NCT01518881
	siRNA-EphA2-DOPC	Advanced malignant solid neoplasm	EphA2	Lipoplex	IV	I	2012	Recruiting	NCT01591356
	Atu027	Pancreatic ductal carcinoma	PKN3	Lipoplex	IV	I/II	2013	Completed	NCT01808638
	TKM-080301	Advanced hepatocellular carcinoma	PLK1	LNP	IV	I/II	2014	Completed	NCT02191878
	TKM-100802	Ebola virus infection	VP24, VP35, L-polymerase	LNP	IV	I	2014	Terminated	NCT02041715
	ARB-001467	Chronic hepatitis B infection	HBV transcripts	LNP	IV	II	2015	Completed	NCT02631096
	DCR-MYC	Hepatocellular carcinoma	MYC	LNP	IV	I/II	2016	Terminated	NCT02314052
	ARB-1740	Chronic hepatitis B infection	HBV transcripts	LNP	IV	Ia/Ib	2017	Terminated	ACTRN12617000557336
	ND-L02-s0201	Idiopathic pulmonary fibrosis	HSP47	LNP	IV	II	2018	Active, recruiting	NCT03538301
mRNA	VAL-506440	Influenza	H10N8 Antigen	LNP	IM	I	2015	Completed	NCT03076385
	mRNA-1325	Zika virus infection	Zika virus antigenic proteins	LNP	IM	I/II	2016	Completed	NCT03014089
	mRNA-2416	Advanced/metastatic solid tumors or lymphoma	OX40L	LNP	Intratumoral injection	I	2017	Recruiting	NCT03323398
	mRNA-4157	Solid tumors	Personalized neoantigens	LNP	IM	I	2017	Active, recruiting	NCT03313778
	MRT5005	Cystic fibrosis	CFTR	LNP	INH	I/II	2018	Active, recruiting	NCT03375047
	MRT5201	Ornithine transcarbamylase deficiency	OTC	LNP	IV	I/II	2019	Withdrawn	NCT03767270
	BNT115	Ovarian cancer	TAAs	Lipoplex	IM	I	2019	Active, not recruiting	NCT04163094
	mRNA-1273	SARS-CoV-2 infection	Full-length, prefusion stabilized spike (S) protein	LNP	IM	I	2020	Active, recruiting	NCT04283461
	MEDI1191	Solid tumors	IL12 mRNA	LNP	IM	I	2019	Active, not recruiting	NCT03946800
miRNA	MRX34	Primary liver cancer; SCLC; lymphoma; melanoma; multiple myeloma; renal cell carcinoma; NSCLC	miR-34	LNP	IV	I	2016	Withdrawn	NCT02862145
ASO	LErafAON-ETU	Advanced cancer	C-raf	LNP	IV	I	2003	Completed	NCT00100672
	BP1001	AML, ALL, MDS, and CML	Grb2 mRNA	Lipoplex	IV	II	2016	Recruiting	NCT02781883
saRNA	MTL-CEBPA	Hepatocellular carcinoma	CEBPA	Lipoplex	IV	I	2016	Recruiting	NCT02716012
anti-miR	Cobomarsen	CTCL, CLL, DLBCL, ABC, ATLL	miRNA-155	LNP	IV	I	2016	Completed	NCT01727934

IV, intravenous; INH, inhalation; IM, intramuscular; AML, acute myeloid leukemia; ACC, adrenocortical carcinoma; NET, neuroendocrine tumor; ALL, acute lymphoblastic leukemia; MDS, myelodysplastic syndrome; CML, chronic myelocytic leukemia; CTCL, cutaneous T-cell lymphoma; CLL, chronic lymphocytic leukemia; DLBCL, diffuse large B-cell lymphoma; ABC, activated B-cell subtype; ATLL, adult T-cell leukemia/lymphoma; SARS-CoV-2, severe acute respiratory syndrome coronavirus 2; SCLC, small cell lung cancer; NSCLC, non-small cell lung cancer.

models without prior exposure to PEG. However, humans are increasingly exposed to numerous PEG-containing marketed products and presumably possess anti-PEG antibodies before they are introduced with liposomes, complicating the situation in the clinical.

8.2. *Targeting beyond the liver*

Of the 26 clinical trials with data in Table 3, 18 were based on intravenous injection, with 9 treatments targeting the liver. The findings from these studies supported the supposition that systemic injection is the best administration route but that targeting sites beyond the liver faces challenges. The liver tropism of lipid nanovehicles is mainly attributed to the following reasons: 1) the blood flow rate through the liver is high, accounting for 27% of cardiac output; 2) sinusoidal membranes in the liver are extensively fenestrated; 3) Kupffer cells, liver-specific macrophages, are responsible for clearing most nanoparticles; and 4) liver endothelial cells present efficient uptake activity[60]. In addition to traditional active and passive targeting tactics, innovative strategies have been developed to achieve targeting sites outside the liver (*e.g.*, targeting the spleen, lung, and tumors), including targeting by adjusting the lipid constituents and physicochemical properties of the lipid nanovehicles and biomimetic decoration.

8.2.1. *Targeting the spleen*

As mentioned above, lipid nanovehicles in the blood circulatory system are opsonized, phagocytosed, and then accumulate in the MPS, including the liver and spleen. However, most injected lipid nanovehicles (~80%) are delivered to the liver. Therefore, some strategies have been developed to modulate the physicochemical properties of lipid nanovehicles and have shown increased spleen tropism. Indeed, the incorporation of cholesterol increased the rigidity of the lipid bilayer[162], thereby promoting its uptake into the spleen[163]. In addition, Kranz et al.[164] prepared a series of lipoplexes with different charge ratios (*i.e.*, different cationic lipid: RNA ratios) without targeting ligands. They observed that gene expression was decreased in the lung and increased in the spleen as the cationic lipid: RNA ratio was gradually decreased, suggesting that the charge ratio may play a crucial role in organ-specific gene expression. Similarly, a recent study reported that adding anionic lipids and the modulation of their molar ratio facilitated a change in the tissue tropism of LNPs, showing reduced delivery rates to the liver and higher delivery rates to the spleen[165].

8.2.2. *Targeting the lung*

Lung-targeted RNA delivery is achieved mainly *via* two strategies: active targeting and passive targeting. In the first approach, lipid nanovehicles are modified with a specific targeting ligand that binds to a specific target receptor on the lung vasculature. Specifically, Parhiz et al.[166] modified mRNA-loaded LNPs with antibodies specifically against platelet endothelial cell adhesion molecule-1 (PECAM-1), which led to lower hepatic uptake and a concomitant increase of ~200-fold in mRNA delivery to the lungs compared to that of their untargeted counterpart. Passive targeting is generally achieved by modulating the physicochemical properties and lipid composition of lipid nanovehicles. McMillan et al.[167] constructed lipoplexes containing DOTAP and DOPE and found that they effectively delivered siRNA to the lung, including epithelial and endothelial cells. At a relatively high siRNA dose of 2 mg/kg, these lipoplexes caused 80% of genes to be silenced at 48 h postinjection. Cheng et al.[165,168] recently developed a selective tissue-targeting strategy termed selective organ targeting (SORT). The SORT LNPs that functionally delivered mRNA to the lung contained a high percentage of permanently cationic lipids, *e.g.*, DOTAP. Including 50% DOTAP into ionizable lipid-containing LNPs effectively tuned their lung-specific tropism. However, since lung tropism was driven by temporal trapping of the LNPs in microvessels accompanied by the formation of large aggregates within erythrocytes, this strategy may cause microinfarction and, therefore, possible myocardial damage and tissue ischemia[169].

8.2.3. *Targeting the tumor*

Most studies have reported that the average intratumoral accumulation of lipid nanovehicles following systemic administration ranges from 5% to 10% (*w*/*w*) of the injected dose, much of which was taken up by the MPS[170,171]. Inspired by nature, bioinspired and biomimetic technology has been used for tumor targeting. As an alternative to a classical PEG coating, red blood cells (RBCs) naturally evade the MPS by triggering an inhibitory molecule of "signal regulatory protein α (SIRPα)" on the surfaces of macrophages. Therefore, incorporating a lipophilic drug into mouse RBCs showed a more than 10-fold longer circulatory time than PEGylated micellar carriers, leading to efficient cargo delivery to tumor tissues[172]. Furthermore, Zhuang's team[173] utilized platelet membranes to wrap siRNA-loaded metal-organic framework (MOF) nanoparticles, which showed ~6-fold higher accumulation in tumors than their RBC membrane-coated counterparts owing to the excellent tumor-targeting ability of the platelet membrane.

9. Conclusions and future perspectives

Although lipid nanovehicles were initially used for RNA delivery in the late 1970s, three LNP-based RNA therapeutics have been approved for marketing in the past five years, suggesting a profound bottleneck in the clinical use of lipid nanovehicles. First, the potency and toxicities of lipid formulations are the most crucial indicators. Fortunately, some high-throughput methods have been developed for lipid synthesis and formulation optimization, facilitating rapid screening of high-potency and low-toxicity lipid formulations. Li et al.[174] designed a three-component reaction system to simplify the tedious lipid synthesis process and rapidly synthesized a library of 720 novel biodegradable ionizable lipids. Kauffman et al.[175] utilized the Design of Experiment (DOE) for LNP formulation optimization and thus considerably reduced the number of individual experiments required to establish statistically significant trends. The resulting LNPs loaded with erythropoietin mRNA showed 7-fold higher potency than the original LNP formulation.

Surface PEGylation increases lipid nanovehicle stability *in vitro* and prolongs lipid nanovehicle retention in blood by preventing the adsorption of plasma proteins and reducing subsequent MPS uptake. However, it also prevents lipid nanovehicles from entering cells and escaping from endosomes (*i.e.*, the PEG dilemma)[79] and leads to rapid elimination of lipid nanovehicles by stimulating B cells to secrete anti-PEG IgM (*i.e.*, the ABC phenomenon)[104–106]. In contrast, biomembrane camouflage reduces MPS uptake of lipid nanovehicles, promotes their cell internalization, and shows little immunogenicity, representing a more appealing strategy[131]. However, no biomimetic lipid nanovehicle-based RNA drugs have yet been approved for use in

the clinical, mainly because of their batch-to-batch variation and lack of scalable production methods[176]. A practical solution to these challenges will inspire the development of biomimetic lipid nanovehicle-based RNA therapeutics.

Due to the liver tropism of lipid nanovehicles, targeting tissues outside the liver is still challenging. Interestingly, SORT LNPs have been shown to target extrahepatic tissues. Cheng et al.[165] reported a SORT strategy in which multiple types of LNPs were engineered by adding a SORT molecule, leading to selective editing of extrahepatic tissues. Patisiran targets the liver following systemic injection. However, when DOTAP (a SORT molecule) was added to the patisiran formulation, the protein expression profile changed; it was decreased in the liver and increased in the spleen and lung[176]. With the development of the SORT technique, lipid nanovehicle-based RNA products used for extrahepatic disease treatment will be available in the clinical in the future.

Acknowledgments

The work was supported by the National Natural Science Foundation of China (Nos. 82172098, 81872428, 81703010, and 82202344) and the Shanghai Municipal Natural Science Foundation (23ZR1463300).

Author contributions

Jing Yan: Writing-original draft, Data curation, Figure design, manuscript revision. Hao Zhang: Figure drawing, manuscript revision. Guangfeng Li: Data curation, Figure design. Jiacan Su, Yan Wei, and Can Xu: Conceptualization, Resources, Supervision, Writing−review & editing, Funding acquisition.

Conflicts of interest

The authors declare no conflicts of interest.

References

1. Miname MH, Rocha VZ, Santos RD. The role of RNA-targeted therapeutics to reduce ASCVD risk: what have we learned recently?. *Curr Atherosclerosis Rep* 2021;**23**:40.
2. Hannon GJ, Rossi JJ. Unlocking the potential of the human genome with RNA interference. *Nature* 2004;**431**:371−8.
3. Roberts TC, Langer R, Wood MJA. Advances in oligonucleotide drug delivery. *Nat Rev Drug Discov* 2020;**19**:673−94.
4. Dowdy SF. Overcoming cellular barriers for RNA therapeutics. *Nat Biotechnol* 2017;**35**:222−9.
5. Buck J, Grossen P, Cullis PR, Huwyler J, Witzigmann D. Lipid-based DNA therapeutics: hallmarks of non-viral gene delivery. *ACS Nano* 2019;**13**:3754−82.
6. Tao Y, Chen Y, Wang S, Chen W, Zhou D, Chen D, et al. Optimizing the modification density of acid oligopeptides to enhance the bone-targeting activity of liposomes. *Compos B Eng* 2022;**247**:110288.
7. Duan N, Li J, Song S, Wang F, Yang Y, Nie D, et al. Enzyme-activated prodrug-based smart liposomes specifically enhance tumor hemoperfusion with efficient drug delivery to pancreatic cancer cells and stellate cells. *Adv Funct Mater* 2021;**31**:2100605.
8. Wei Y, Song S, Duan N, Wang F, Wang Y, Yang Y, et al. MT1-MMP-activated liposomes to improve tumor blood perfusion and drug delivery for enhanced pancreatic cancer therapy. *Adv Sci* 2020;**7**:1902746.
9. Wei Y, Wang Y, Xia D, Guo S, Wang F, Zhang X, et al. Thermosensitive liposomal codelivery of HSA-paclitaxel and HSA-ellagic acid complexes for enhanced drug perfusion and efficacy against pancreatic cancer. *ACS Appl Mater Interfaces* 2017;**9**:25138−51.
10. Dimitriadis GJ. Entrapment of ribonucleic acids in liposomes. *FEBS Lett* 1978;**86**:289−93.
11. Semple SC, Klimuk SK, Harasym TO, Dos SN, Ansell SM, Wong KF, et al. Efficient encapsulation of antisense oligonucleotides in lipid vesicles using ionizable aminolipids: formation of novel small multilamellar vesicle structures. *Biochim Biophys Acta* 2001;**1510**:152−66.
12. Samaridou E, Heyes J, Lutwyche P. Lipid nanoparticles for nucleic acid delivery: current perspectives. *Adv Drug Deliv Rev* 2020;**154**−**155**:37−63.
13. Khurana A, Allawadhi P, Khurana I, Allwadhi S, Weiskirchen R, Banothu AK, et al. Role of nanotechnology behind the success of mRNA vaccines for COVID-19. *Nano Today* 2021;**38**:101142.
14. Xu C, Wang J. Delivery systems for siRNA drug development in cancer therapy. *Asian J Pharm Sci* 2015;**10**:1−12.
15. Kowalski PS, Rudra A, Miao L, Anderson DG. Delivering the messenger: advances in technologies for therapeutic mRNA delivery. *Mol Ther* 2019;**27**:710−28.
16. Zhang X, Hai L, Gao Y, Yu G, Sun Y. Lipid nanomaterials-based RNA therapy and cancer treatment. *Acta Pharm Sin B* 2023;**13**:903−15.
17. Zhong Y, Du S, Dong Y. MRNA delivery in cancer immunotherapy. *Acta Pharm Sin B* 2023;**13**:1348−57.
18. Charbe NB, Amnerkar ND, Ramesh B, Tambuwala MM, Bakshi HA, Aljabali A, et al. Small interfering RNA for cancer treatment: overcoming hurdles in delivery. *Acta Pharm Sin B* 2020;**10**:2075−109.
19. Gao J, Xia Z, Vohidova D, Joseph J, Luo JN, Joshi N. Progress in non-viral localized delivery of siRNA therapeutics for pulmonary diseases. *Acta Pharm Sin B* 2023;**13**:1400−28.
20. Zoulikha M, Xiao Q, Boafo GF, Sallam MA, Chen Z, He W. Pulmonary delivery of siRNA against acute lung injury/acute respiratory distress syndrome. *Acta Pharm Sin B* 2022;**12**:600−20.
21. Li Y, Ye Z, Yang H, Xu Q. Tailoring combinatorial lipid nanoparticles for intracellular delivery of nucleic acids, proteins, and drugs. *Acta Pharm Sin B* 2022;**12**:2624−39.
22. Manjunath N, Wu H, Subramanya S, Shankar P. Lentiviral delivery of short hairpin RNAs. *Adv Drug Deliv Rev* 2009;**61**:732−45.
23. Aguiar S, van der Gaag B, Cortese FAB. RNAi mechanisms in Huntington' s disease therapy: siRNA *versus* shRNA. *Transl Neurodegener* 2017;**6**:30.
24. Weng Y, Xiao H, Zhang J, Liang X, Huang Y. RNAi therapeutic and its innovative biotechnological evolution. *Biotechnol Adv* 2019;**37**:801−25.
25. Golden RJ, Chen B, Li T, Braun J, Manjunath H, Chen X, et al. An argonaute phosphorylation cycle promotes microRNA-mediated silencing. *Nature* 2017;**542**:197−202.
26. Stenvang J, Kauppinen S. MicroRNAs as targets for antisense-based therapeutics. *Expet Opin Biol Ther* 2008;**8**:59−81.
27. Tarn W, Cheng Y, Ko S, Huang L. Antisense oligonucleotide-based therapy of viral infections. *Pharmaceutics* 2021;**13**:2015.
28. Liang XH, Sun H, Nichols JG, Crooke ST. RNase H1-dependent antisense oligonucleotides are robustly active in directing RNA cleavage in both the cytoplasm and the nucleus. *Mol Ther* 2017;**25**:2075−92.
29. Lima WF, De Hoyos CL, Liang XH, Crooke ST. RNA cleavage products generated by antisense oligonucleotides and siRNAs are processed by the RNA surveillance machinery. *Nucleic Acids Res* 2016;**44**:3351−63.
30. Portnoy V, Lin SH, Li KH, Burlingame A, Hu ZH, Li H, et al. SaRNA-guided Ago2 targets the RITA complex to promoters to stimulate transcription. *Cell Res* 2016;**26**:320−35.
31. Kwok A, Raulf N, Habib N. Developing small activating RNA as a therapeutic: current challenges and promises. *Ther Deliv* 2019;**10**:151−64.

32. Kang MR, Yang G, Place RF, Charisse K, Epstein-Barash H, Manoharan M, et al. Intravesical delivery of small activating RNA formulated into lipid nanoparticles inhibits orthotopic bladder tumor growth. *Cancer Res* 2012;**72**:5069−79.
33. Liang X, Li D, Leng S, Zhu X. RNA-based pharmacotherapy for tumors: from bench to clinic and back. *Biomed Pharmacother* 2020; **125**:109997.
34. Sorrentino S. Human extracellular ribonucleases: multiplicity, molecular diversity and catalytic properties of the major RNase types. *Cell Mol Life Sci* 1998;**54**:785−94.
35. Van de Water FM, Boerman OC, Wouterse AC, Peters JG, Russel FG, Masereeuw R. Intravenously administered short interfering RNA accumulates in the kidney and selectively suppresses gene function in renal proximal tubules. *Drug Metab Dispos* 2006;**34**:1393−7.
36. Wartiovaara J, Ofverstedt LG, Khoshnoodi J, Zhang J, Makela E, Sandin S, et al. Nephrin strands contribute to a porous slit diaphragm scaffold as revealed by electron tomography. *J Clin Invest* 2004;**114**: 1475−83.
37. Mosser DM, Edwards JP. Exploring the full spectrum of macrophage activation. *Nat Rev Immunol* 2008;**8**:958−69.
38. Rappoport JZ. Focusing on clathrin-mediated endocytosis. *Biochem J* 2008;**412**:415−23.
39. Zhao F, Zhao Y, Liu Y, Chang X, Chen C, Zhao Y. Cellular uptake, intracellular trafficking, and cytotoxicity of nanomaterials. *Small* 2011;**7**:1322−37.
40. Dominska M, Dykxhoorn DM. Breaking down the barriers: siRNA delivery and endosome escape. *J Cell Sci* 2010;**123**:1183−9.
41. Varkouhi AK, Scholte M, Storm G, Haisma HJ. Endosomal escape pathways for delivery of biologicals. *J Control Release* 2011;**151**: 220−8.
42. Filion MC, Phillips NC. Toxicity and immunomodulatory activity of liposomal vectors formulated with cationic lipids toward immune effector cells. *Biochim Biophys Acta* 1997;**1329**:345−56.
43. Wan C, Allen TM, Cullis PR. Lipid nanoparticle delivery systems for siRNA-based therapeutics. *Drug Deliv Transl Res* 2014;**4**:74−83.
44. Lappalainen K, Jaaskelainen I, Syrjanen K, Urtti A, Syrjanen S. Comparison of cell proliferation and toxicity assays using two cationic liposomes. *Pharm Res (N Y)* 1994;**11**:1127−31.
45. Mintzer MA, Simanek EE. Nonviral vectors for gene delivery. *Chem Rev* 2009;**109**:259−302.
46. Dokka S, Toledo D, Shi X, Castranova V, Rojanasakul Y. Oxygen radical-mediated pulmonary toxicity induced by some cationic liposomes. *Pharm Res (N Y)* 2000;**17**:521−5.
47. Ruysschaert JM, El OA, Willeaume V, Huez G, Fuks R, Vandenbranden M, et al. A novel cationic amphiphile for transfection of mammalian cells. *Biochem Biophys Res Commun* 1994;**203**: 1622−8.
48. Santel A, Aleku M, Keil O, Endruschat J, Esche V, Fisch G, et al. A novel sirna-lipoplex technology for RNA interference in the mouse vascular endothelium. *Gene Ther* 2006;**13**:1222−34.
49. Santel A, Aleku M, Roder N, Mopert K, Durieux B, Janke O, et al. Atu027 prevents pulmonary metastasis in experimental and spontaneous mouse metastasis models. *Clin Cancer Res* 2010;**16**:5469−80.
50. Aleku M, Schulz P, Keil O, Santel A, Schaeper U, Dieckhoff B, et al. Atu027, a liposomal small interfering RNA formulation targeting protein kinase N3, inhibits cancer progression. *Cancer Res* 2008;**68**:9788−98.
51. Schultheis B, Strumberg D, Kuhlmann J, Wolf M, Link K, Seufferlein T, et al. A phase Ib/IIa study of combination therapy with gemcitabine and Atu027 in patients with locally advanced or metastatic pancreatic adenocarcinoma. *J Clin Oncol* 2016;**34**:385.
52. Banerjee R, Mahidhar YV, Chaudhuri A, Gopal V, Rao NM. Design, synthesis, and transfection biology of novel cationic glycolipids for use in liposomal gene delivery. *J Med Chem* 2001;**44**:4176−85.
53. Chen Y, Sen J, Bathula SR, Yang Q, Fittipaldi R, Huang L. Novel cationic lipid that delivers siRNA and enhances therapeutic effect in lung cancer cells. *Mol Pharm* 2009;**6**:696−705.
54. Liu Q, Jiang QQ, Yi WJ, Zhang J, Zhang XC, Wu MB, et al. Novel imidazole-functionalized cyclen cationic lipids: synthesis and application as non-viral gene vectors. *Bioorg Med Chem* 2013;**21**: 3105−13.
55. Hafez IM, Maurer N, Cullis PR. On the mechanism whereby cationic lipids promote intracellular delivery of polynucleic acids. *Gene Ther* 2001;**8**:1188−96.
56. Heyes J, Palmer L, Bremner K, Maclachlan I. Cationic lipid saturation influences intracellular delivery of encapsulated nucleic acids. *J Control Release* 2005;**107**:276−87.
57. Zimmermann TS, Lee AC, Akinc A, Bramlage B, Bumcrot D, Fedoruk MN, et al. RNAi-mediated gene silencing in non-human primates. *Nature* 2006;**441**:111−4.
58. Semple SC, Akinc A, Chen J, Sandhu AP, Mui BL, Cho CK, et al. Rational design of cationic lipids for siRNA delivery. *Nat Biotechnol* 2010;**28**:172−6.
59. Jayaraman M, Ansell SM, Mui BL, Tam YK, Chen J, Du X, et al. Maximizing the potency of siRNA lipid nanoparticles for hepatic gene silencing *in vivo*. *Angew Chem Int Ed Engl* 2012;**51**:8529−33.
60. Akinc A, Maier MA, Manoharan M, Fitzgerald K, Jayaraman M, Barros S, et al. The Onpattro story and the clinical translation of nanomedicines containing nucleic acid-based drugs. *Nat Nanotechnol* 2019;**14**:1084−7.
61. Sabnis S, Kumarasinghe ES, Salerno T, Mihai C, Ketova T, Senn JJ, et al. A novel amino lipid series for mRNA delivery: improved endosomal escape and sustained pharmacology and safety in non-human primates. *Mol Ther* 2018;**26**:1509−19.
62. Love KT, Mahon KP, Levins CG, Whitehead KA, Querbes W, Dorkin JR, et al. Lipid-like materials for low-dose, *in vivo* gene silencing. *Proc Natl Acad Sci U S A* 2010;**107**:1864−9.
63. Akinc A, Zumbuehl A, Goldberg M, Leshchiner ES, Busini V, Hossain N, et al. A combinatorial library of lipid-like materials for delivery of RNAi therapeutics. *Nat Biotechnol* 2008;**26**:561−9.
64. Cho SW, Goldberg M, Son SM, Xu Q, Yang F, Mei Y, et al. Lipid-like nanoparticles for small interfering RNA delivery to endothelial cells. *Adv Funct Mater* 2009;**19**:3112−8.
65. Witzigmann D, Kulkarni JA, Leung J, Chen S, Cullis PR, van der Meel R. Lipid nanoparticle technology for therapeutic gene regulation in the liver. *Adv Drug Deliv Rev* 2020;**159**:344−63.
66. Yan X, Scherphof GL, Kamps JA. Liposome opsonization. *J Liposome Res* 2005;**15**:109−39.
67. May S, Harries D, Ben-Shaul A. The phase behavior of cationic lipid-DNA complexes. *Biophys J* 2000;**78**:1681−97.
68. Hattori Y, Suzuki S, Kawakami S, Yamashita F, Hashida M. The role of dioleoylphosphatidylethanolamine (DOPE) in targeted gene delivery with mannosylated cationic liposomes *via* intravenous route. *J Control Release* 2005;**108**:484−95.
69. Zhang Y, Sun C, Wang C, Jankovic KE, Dong Y. Lipids and lipid derivatives for RNA delivery. *Chem Rev* 2021;**121**:12181−277.
70. Kulkarni JA, Witzigmann D, Leung J, Tam Y, Cullis PR. On the role of helper lipids in lipid nanoparticle formulations of siRNA. *Nanoscale* 2019;**11**:21733−9.
71. Sakurai F, Nishioka T, Yamashita F, Takakura Y, Hashida M. Effects of erythrocytes and serum proteins on lung accumulation of lipoplexes containing cholesterol or DOPE as a helper lipid in the single-pass rat lung perfusion system. *Eur J Pharm Biopharm* 2001; **52**:165−72.
72. Wang T, Larcher LM, Ma L, Veedu RN. Systematic screening of commonly used commercial transfection reagents towards efficient transfection of Single-Stranded oligonucleotides. *Molecules* 2018;**23**: 2564.
73. Nakase I, Niwa M, Takeuchi T, Sonomura K, Kawabata N, Koike Y, et al. Cellular uptake of arginine-rich peptides: roles for macropinocytosis and actin rearrangement. *Mol Ther* 2004;**10**:1011−22.
74. Kaczmarek JC, Kowalski PS, Anderson DG. Advances in the delivery of RNA therapeutics: from concept to clinical reality. *Genome Med* 2017;**9**:60.
75. Kirby C, Clarke J, Gregoriadis G. Effect of the cholesterol content of small unilamellar liposomes on their stability *in vivo* and *in vitro*. *Biochem J* 1980;**186**:591−8.

76. Pozzi D, Marchini C, Cardarelli F, Amenitsch H, Garulli C, Bifone A, et al. Transfection efficiency boost of cholesterol-containing lipoplexes. *Biochim Biophys Acta* 2012;**1818**:2335−43.
77. Dabkowska AP, Barlow DJ, Hughes AV, Campbell RA, Quinn PJ, Lawrence MJ. The effect of neutral helper lipids on the structure of cationic lipid monolayers. *J R Soc Interface* 2012;**9**:548−61.
78. Semple SC, Chonn A, Cullis PR. Influence of cholesterol on the association of plasma proteins with liposomes. *Biochemistry-Us* 1996;**35**:2521−5.
79. Gomes-Da-Silva LC, Fonseca NA, Moura V, Pedroso DLM, Simões S, Moreira JN. Lipid-based nanoparticles for siRNA delivery in cancer therapy: paradigms and challenges. *Acc Chem Res* 2012;**45**:1163−71.
80. Belliveau NM, Huft J, Lin PJ, Chen S, Leung AK, Leaver TJ, et al. Microfluidic synthesis of highly potent limit-size lipid nanoparticles for *in vivo* delivery of siRNA. *Mol Ther Nucleic Acids* 2012;**1**:e37.
81. Li SD, Chono S, Huang L. Efficient gene silencing in metastatic tumor by siRNA formulated in surface-modified nanoparticles. *J Control Release* 2008;**126**:77−84.
82. Kim SI, Shin D, Lee H, Ahn BY, Yoon Y, Kim M. Targeted delivery of siRNA against hepatitis C virus by apolipoprotein A-I-bound cationic liposomes. *J Hepatol* 2009;**50**:479−88.
83. Tagami T, Nakamura K, Shimizu T, Ishida T, Kiwada H. Effect of siRNA in PEG-coated siRNA-lipoplex on anti-PEG IgM production. *J Control Release* 2009;**137**:234−40.
84. Carmona S, Jorgensen MR, Kolli S, Crowther C, Salazar FH, Marion PL, et al. Controlling HBV replication *in vivo* by intravenous administration of triggered PEGylated siRNA-nanoparticles. *Mol Pharm* 2009;**6**:706−17.
85. Buyens K, Demeester J, De Smedt SS, Sanders NN. Elucidating the encapsulation of short interfering RNA in PEGylated cationic liposomes. *Langmuir* 2009;**25**:4886−91.
86. Gao K, Huang L. Nonviral methods for siRNA delivery. *Mol Pharm* 2009;**6**:651−8.
87. Li J, Chen Y, Tseng Y, Mozumdar S, Huang L. Biodegradable calcium phosphate nanoparticle with lipid coating for systemic siRNA delivery. *J Control Release* 2010;**142**:416−21.
88. Kulkarni JA, Darjuan MM, Mercer JE, Chen S, van der Meel R, Thewalt JL, et al. On the formation and morphology of lipid nanoparticles containing ionizable cationic lipids and siRNA. *ACS Nano* 2018;**12**:4787−95.
89. Leung AK, Hafez IM, Baoukina S, Belliveau NM, Zhigaltsev IV, Afshinmanesh E, et al. Lipid nanoparticles containing siRNA synthesized by microfluidic mixing exhibit an Electron-Dense nanostructured core. *J Phys Chem C Nanomater Interfaces* 2012;**116**:18440−50.
90. Tenchov R, Bird R, Curtze AE, Zhou Q. Lipid nanoparticles—from liposomes to mRNA vaccine delivery, a landscape of research diversity and advancement. *ACS Nano* 2021;**15**:16982−7015.
91. Weisman S, Hirsch-Lerner D, Barenholz Y, Talmon Y. Nanostructure of cationic lipid-oligonucleotide complexes. *Biophys J* 2004;**87**:609−14.
92. Lee H, Lytton-Jean AK, Chen Y, Love KT, Park AI, Karagiannis ED, et al. Molecularly self-assembled nucleic acid nanoparticles for targeted *in vivo* siRNA delivery. *Nat Nanotechnol* 2012;**7**:389−93.
93. Lin Q, Chen J, Zhang Z, Zheng G. Lipid-based nanoparticles in the systemic delivery of siRNA. *Nanomedicine* 2014;**9**:105−20.
94. Geisbert TW, Lee AC, Robbins M, Geisbert JB, Honko AN, Sood V, et al. Postexposure protection of non-human primates against a lethal Ebola virus challenge with RNA interference: a proof-of-concept study. *Lancet* 2010;**375**:1896−905.
95. Morrissey DV, Lockridge JA, Shaw L, Blanchard K, Jensen K, Breen W, et al. Potent and persistent *in vivo* anti-HBV activity of chemically modified siRNAs. *Nat Biotechnol* 2005;**23**:1002−7.
96. Evers M, van de Wakker SI, de Groot EM, de Jong OG, Gitz-Francois J, Seinen CS, et al. Functional sirna delivery by extracellular vesicle-liposome hybrid nanoparticles. *Adv Healthcare Mater* 2022;**11**:e2101202.
97. Buyens K, De Smedt SC, Braeckmans K, Demeester J, Peeters L, van Grunsven LA, et al. Liposome based systems for systemic siRNA delivery: stability in blood sets the requirements for optimal carrier design. *J Control Release* 2012;**158**:362−70.
98. Hatakeyama H, Akita H, Ito E, Hayashi Y, Oishi M, Nagasaki Y, et al. Systemic delivery of siRNA to tumors using a lipid nanoparticle containing a tumor-specific cleavable PEG-lipid. *Biomaterials* 2011;**32**:4306−16.
99. Li J, Yang Y, Huang L. Calcium phosphate nanoparticles with an asymmetric lipid bilayer coating for sirna delivery to the tumor. *J Control Release* 2012;**158**:108−14.
100. Garbuzenko O, Barenholz Y, Priev A. Effect of grafted PEG on liposome size and on compressibility and packing of lipid bilayer. *Chem Phys Lipids* 2005;**135**:117−29.
101. Xu Y, Shi L, Deng YH. Effect of polyethylene glycol-lipid derivatives on the stability of grafted liposomes. *Yao Xue Xue Bao* 2011;**46**:1178−86.
102. Owensiii D, Peppas N. Opsonization, biodistribution, and pharmacokinetics of polymeric nanoparticles. *Int J Pharm* 2006;**307**:93−102.
103. Barattin M, Mattarei A, Balasso A, Paradisi C, Cantù L, Del FE, et al. pH-Controlled liposomes for enhanced cell penetration in tumor environment. *ACS Appl Mater Interfaces* 2018;**10**:17646−61.
104. Hsieh YC, Wang HE, Lin WW, Roffler SR, Cheng TC, Su YC, et al. Pre-existing anti-polyethylene glycol antibody reduces the therapeutic efficacy and pharmacokinetics of PEGylated liposomes. *Theranostics* 2018;**8**:3164−75.
105. Abu Lila AS, Kiwada H, Ishida T. The accelerated blood clearance (ABC) phenomenon: clinical challenge and approaches to manage. *J Control Release* 2013;**172**:38−47.
106. Laverman P, Carstens MG, Boerman OC, Dams ET, Oyen WJ, van Rooijen N, et al. Factors affecting the accelerated blood clearance of polyethylene glycol-liposomes upon repeated injection. *J Pharmacol Exp Therapeut* 2001;**298**:607−12.
107. Rao J. Shedding light on tumors using nanoparticles. *ACS Nano* 2008;**2**:1984−6.
108. Devine DV, Wong K, Serrano K, Chonn A, Cullis PR. Liposome-complement interactions in rat serum: implications for liposome survival studies. *Biochim Biophys Acta* 1994;**1191**:43−51.
109. Harashima H, Sakata K, Funato K, Kiwada H. Enhanced hepatic uptake of liposomes through complement activation depending on the size of liposomes. *Pharm Res (N Y)* 1994;**11**:402−6.
110. Yoo JW, Chambers E, Mitragotri S. Factors that control the circulation time of nanoparticles in blood: challenges, solutions and future prospects. *Curr Pharmaceut Des* 2010;**16**:2298−307.
111. Bertrand N, Leroux J. The journey of a drug-carrier in the body: an anatomo-physiological perspective. *J Control Release* 2012;**161**:152−63.
112. Al-Ahmady Z, Kostarelos K. Chemical components for the design of temperature-responsive vesicles as cancer therapeutics. *Chem Rev* 2016;**116**:3883−918.
113. Needham D, Nunn RS. Elastic deformation and failure of lipid bilayer membranes containing cholesterol. *Biophys J* 1990;**58**:997−1009.
114. Webb MS, Harasym TO, Masin D, Bally MB, Mayer LD. Sphingomyelin-cholesterol liposomes significantly enhance the pharmacokinetic and therapeutic properties of vincristine in murine and human tumour models. *Br J Cancer* 1995;**72**:896−904.
115. Saunders NRM, Paolini MS, Fenton OS, Poul L, Devalliere J, Mpambani F, et al. A nanoprimer to improve the systemic delivery of siRNA and mRNA. *Nano Lett* 2020;**20**:4264−9.
116. Noble GT, Stefanick JF, Ashley JD, Kiziltepe T, Bilgicer B. Ligand-targeted liposome design: challenges and fundamental considerations. *Trends Biotechnol* 2014;**32**:32−45.
117. Wu J, Nantz MH, Zern MA. Targeting hepatocytes for drug and gene delivery: emerging novel approaches and applications. *Front Biosci* 2002;**7**:d717−25.

118. Kawakami S, Fumoto S, Nishikawa M, Yamashita F, Hashida M. *In vivo* gene delivery to the liver using novel galactosylated cationic liposomes. *Pharm Res (N Y)* 2000;**17**:306−13.
119. Sonoke S, Ueda T, Fujiwara K, Kuwabara K, Yano J. Galactose-modified cationic liposomes as a liver-targeting delivery system for small interfering RNA. *Biol Pharm Bull* 2011;**34**:1338−42.
120. Sawant RR, Torchilin VP. Challenges in development of targeted liposomal therapeutics. *AAPS J* 2012;**14**:303−15.
121. Willis M, Forssen E. Ligand-targeted liposomes. *Adv Drug Deliv Rev* 1998;**29**:249−71.
122. Ruoslahti E. Peptides as targeting elements and tissue penetration devices for nanoparticles. *Adv Mater* 2012;**24**:3747−56.
123. Khabazian E, Vakhshiteh F, Norouzi P, Fatahi Y, Dinarvand R, Atyabi F. Cationic liposome decorated with cyclic RGD peptide for targeted delivery of anti-STAT3 siRNA to melanoma cancer cells. *J Drug Target* 2022;**30**:522−33.
124. Yang ZZ, Li JQ, Wang ZZ, Dong DW, Qi XR. Tumor-targeting dual peptides-modified cationic liposomes for delivery of siRNA and docetaxel to gliomas. *Biomaterials* 2014;**35**:5226−39.
125. Goren D, Horowitz AT, Zalipsky S, Woodle MC, Yarden Y, Gabizon A. Targeting of stealth liposomes to erbB-2 (Her/2) receptor: *in vitro* and *in vivo* studies. *Br J Cancer* 1996;**74**: 1749−56.
126. Gabizon A, Horowitz AT, Goren D, Tzemach D, Shmeeda H, Zalipsky S. *In vivo* fate of folate-targeted polyethylene-glycol liposomes in tumor-bearing mice. *Clin Cancer Res* 2003;**9**: 6551−9.
127. Zhou Z, Liu X, Zhu D, Wang Y, Zhang Z, Zhou X, et al. Nonviral cancer gene therapy: delivery cascade and vector nanoproperty integration. *Adv Drug Deliv Rev* 2017;**115**:115−54.
128. Cao J, Yang P, Wang P, Xu S, Cheng Y, Qian K, et al. 'Adhesion and release' nanoparticle-mediated efficient inhibition of platelet activation disrupts endothelial barriers for enhanced drug delivery in tumors. *Biomaterials* 2020;**269**:120620.
129. Kim B, Pang H, Kang J, Park J, Ruoslahti E, Sailor MJ. Immunogene therapy with fusogenic nanoparticles modulates macrophage response to Staphylococcus aureus. *Nat Commun* 2018;**9**:1969.
130. Kim B, Sun S, Varner JA, Howell SB, Ruoslahti E, Sailor MJ. Securing the payload, finding the cell, and avoiding the endosome: peptide-targeted, fusogenic porous silicon nanoparticles for delivery of siRNA. *Adv Mater* 2019;**31**:1902952.
131. Wu Z, Zhang H, Yan J, Wei Y, Su J. Engineered biomembrane-derived nanoparticles for nanoscale theranostics. *Theranostics* 2023;**13**:20−39.
132. Chen Z, Zhao P, Luo Z, Zheng M, Tian H, Gong P, et al. Cancer cell membrane-biomimetic nanoparticles for homologous-targeting dual-modal imaging and photothermal therapy. *ACS Nano* 2016;**10**: 10049−57.
133. Liu Z, Wang F, Liu X, Sang Y, Zhang L, Ren J, et al. Cell membrane−camouflaged liposomes for tumor cell−selective glycans engineering and imaging *in vivo*. *Proc Natl Acad Sci U S A* 2021;**118**: e2022769118.
134. Sahay G, Querbes W, Alabi C, Eltoukhy A, Sarkar S, Zurenko C, et al. Efficiency of siRNA delivery by lipid nanoparticles is limited by endocytic recycling. *Nat Biotechnol* 2013;**31**:653−8.
135. Gilleron J, Querbes W, Zeigerer A, Borodovsky A, Marsico G, Schubert U, et al. Image-based analysis of lipid nanoparticle-mediated siRNA delivery, intracellular trafficking and endosomal escape. *Nat Biotechnol* 2013;**31**:638−46.
136. Yanez Arteta M, Kjellman T, Bartesaghi S, Wallin S, Wu X, Kvist AJ, et al. Successful reprogramming of cellular protein production through mRNA delivered by functionalized lipid nanoparticles. *Proc Natl Acad Sci U S A* 2018;**115**:E3351−60.
137. Wasungu L, Hoekstra D. Cationic lipids, lipoplexes and intracellular delivery of genes. *J Control Release* 2006;**116**:255−64.
138. Hoekstra D, Rejman J, Wasungu L, Shi F, Zuhorn I. Gene delivery by cationic lipids: in and out of an endosome. *Biochem Soc Trans* 2007; **35**:68−71.
139. Martens TF, Remaut K, Demeester J, De Smedt SC, Braeckmans K. Intracellular delivery of nanomaterials: how to catch endosomal escape in the act. *Nano Today* 2014;**9**:344−64.
140. Miura N, Shaheen SM, Akita H, Nakamura T, Harashima H. A KALA-modified lipid nanoparticle containing CpG-free plasmid DNA as a potential DNA vaccine carrier for antigen presentation and as an immune-stimulative adjuvant. *Nucleic Acids Res* 2015;**43**: 1317−31.
141. Mundra V, Mahato RI. Design of nanocarriers for efficient cellular uptake and endosomal release of small molecule and nucleic acid drugs: learning from virus. *Front Chem Sci Eng* 2014;**8**:387−404.
142. Ermilova I, Swenson J. DOPC *versus* DOPE as a helper lipid for gene-therapies: molecular dynamics simulations with DLin-MC3-DMA. *Phys Chem Chem Phys* 2020;**22**:28256−68.
143. Zhang X, Goel V, Robbie GJ. Pharmacokinetics of patisiran, the first approved RNA interference therapy in patients with hereditary transthyretin-Mediated amyloidosis. *J Clin Pharmacol* 2020;**60**: 573−85.
144. Suzuki Y, Ishihara H. Difference in the lipid nanoparticle technology employed in three approved siRNA (Patisiran) and mRNA (COVID-19 vaccine) drugs. *Drug Metabol Pharmacokinet* 2021; **41**:100424.
145. Lv H, Zhang S, Wang B, Cui S, Yan J. Toxicity of cationic lipids and cationic polymers in gene delivery. *J Control Release* 2006;**114**: 100−9.
146. Kormann MS, Hasenpusch G, Aneja MK, Nica G, Flemmer AW, Herber-Jonat S, et al. Expression of therapeutic proteins after delivery of chemically modified mRNA in mice. *Nat Biotechnol* 2011; **29**:154−7.
147. Marques JT, Williams BR. Activation of the mammalian immune system by siRNAs. *Nat Biotechnol* 2005;**23**:1399−405.
148. Judge AD, Sood V, Shaw JR, Fang D, Mcclintock K, Maclachlan I. Sequence-dependent stimulation of the mammalian innate immune response by synthetic siRNA. *Nat Biotechnol* 2005;**23**:457−62.
149. Medzhitov R, Janeway CJ. Decoding the patterns of self and nonself by the innate immune system. *Science* 2002;**296**:298−300.
150. Broering R, Real CI, John MJ, Jahn-Hofmann K, Ickenstein LM, Kleinehr K, et al. Chemical modifications on siRNAs avoid Toll-like-receptor-mediated activation of the hepatic immune system *in vivo* and *in vitro*. *Int Immunol* 2014;**26**:35−46.
151. Andries O, Mc CS, De Smedt SC, Weiss R, Sanders NN, Kitada T. N^1-methylpseudouridine-incorporated mRNA outperforms pseudouridine-incorporated mRNA by providing enhanced protein expression and reduced immunogenicity in mammalian cell lines and mice. *J Control Release* 2015;**217**:337−44.
152. Abrams MT, Koser ML, Seitzer J, Williams SC, Dipietro MA, Wang W, et al. Evaluation of efficacy, biodistribution, and inflammation for a potent siRNA nanoparticle: effect of dexamethasone co-treatment. *Mol Ther* 2010;**18**:171−80.
153. Sedic M, Senn JJ, Lynn A, Laska M, Smith M, Platz SJ, et al. Safety evaluation of lipid nanoparticle-formulated modified mRNA in the Sprague−Dawley rat and cynomolgus monkey. *Vet Pathol* 2018;**55**: 341−54.
154. Szebeni J. Complement activation-related pseudoallergy: a stress reaction in blood triggered by nanomedicines and biologicals. *Mol Immunol* 2014;**61**:163−73.
155. Kumar V, Qin J, Jiang Y, Duncan RG, Brigham B, Fishman S, et al. Shielding of lipid nanoparticles for siRNA delivery: impact on physicochemical properties, cytokine induction, and efficacy. *Mol Ther Nucleic Acids* 2014;**3**:e210.
156. Giles AJ, Hutchinson M, Sonnemann HM, Jung J, Fecci PE, Ratnam NM, et al. Dexamethasone-induced immunosuppression: mechanisms and implications for immunotherapy. *J Immunother Cancer* 2018;**6**:51.
157. Coelho T, Adams D, Silva A, Lozeron P, Hawkins PN, Mant T, et al. Safety and efficacy of RNAi therapy for transthyretin amyloidosis. *N Engl J Med* 2013;**369**:819−29.

158. Seif F, Khoshmirsafa M, Aazami H, Mohsenzadegan M, Sedighi G, Bahar M. The role of JAK-STAT signaling pathway and its regulators in the fate of T helper cells. *Cell Commun Signal* 2017;**15**:23.
159. Tao W, Mao X, Davide JP, Ng B, Cai M, Burke PA, et al. Mechanistically probing lipid-siRNA nanoparticle-associated toxicities identifies Jak inhibitors effective in mitigating multifaceted toxic responses. *Mol Ther* 2011;**19**:567−75.
160. Reid KB, Porter RR. The proteolytic activation systems of complement. *Annu Rev Biochem* 1981;**50**:433−64.
161. Judge A, Mcclintock K, Phelps JR, Maclachlan I. Hypersensitivity and loss of disease site targeting caused by antibody responses to PEGylated liposomes. *Mol Ther* 2006;**13**:328−37.
162. De Meyer F, Smit B. Effect of cholesterol on the structure of a phospholipid bilayer. *Proc Natl Acad Sci U S A* 2009;**106**:3654−8.
163. Moghimi SM, Patel HM. Serum opsonins and phagocytosis of saturated and unsaturated phospholipid liposomes. *Biochim Biophys Acta* 1989;**984**:384−7.
164. Kranz LM, Diken M, Haas H, Kreiter S, Loquai C, Reuter KC, et al. Systemic RNA delivery to dendritic cells exploits antiviral defence for cancer immunotherapy. *Nature* 2016;**534**:396−401.
165. Cheng Q, Wei T, Farbiak L, Johnson LT, Dilliard SA, Siegwart DJ. Selective organ targeting (SORT) nanoparticles for tissue-specific mRNA delivery and CRISPR-Cas gene editing. *Nat Nanotechnol* 2020;**15**:313−20.
166. Parhiz H, Shuvaev VV, Pardi N, Khoshnejad M, Kiseleva RY, Brenner JS, et al. PECAM-1 directed re-targeting of exogenous mRNA providing two orders of magnitude enhancement of vascular delivery and expression in lungs independent of apolipoprotein E-mediated uptake. *J Control Release* 2018;**291**:106−15.
167. Mccaskill J, Singhania R, Burgess M, Allavena R, Wu S, Blumenthal A, et al. Efficient biodistribution and gene silencing in the lung epithelium *via* intravenous liposomal delivery of siRNA. *Mol Ther Nucleic Acids* 2013;**2**:e96.
168. Liu S, Cheng Q, Wei T, Yu X, Johnson LT, Farbiak L, et al. Membrane-destabilizing ionizable phospholipids for organ-selective mRNA delivery and CRISPR-Cas gene editing. *Nat Mater* 2021;**20**:701−10.
169. Sahin U, Oehm P, Derhovanessian E, Jabulowsky RA, Vormehr M, Gold M, et al. An RNA vaccine drives immunity in checkpoint-inhibitor-treated melanoma. *Nature* 2020;**585**:107−12.
170. Nunes SS, Fernandes RS, Cavalcante CH, Da CCI, Leite EA, Lopes S, et al. Influence of PEG coating on the biodistribution and tumor accumulation of pH-sensitive liposomes. *Drug Deliv Transl Res* 2019;**9**:123−30.
171. Sakurai Y, Hatakeyama H, Sato Y, Hyodo M, Akita H, Harashima H. Gene silencing *via* RNAi and siRNA quantification in tumor tissue using MEND, a liposomal siRNA delivery system. *Mol Ther* 2013;**21**:1195−203.
172. Kim MW, Kwon SH, Choi JH, Lee A. A promising biocompatible platform: lipid-based and bio-inspired smart drug delivery systems for cancer therapy. *Int J Mol Sci* 2018;**19**:3858.
173. Zhuang J, Gong H, Zhou J, Zhang Q, Gao W, Fang RH, et al. Targeted gene silencing *in vivo* by platelet membrane-coated metal-organic framework nanoparticles. *Sci Adv* 2020;**6**:eaaz6108.
174. Li B, Manan RS, Liang SQ, Gordon A, Jiang A, Varley A, et al. Combinatorial design of nanoparticles for pulmonary mRNA delivery and genome editing. *Nat Biotechnol* 2023;**41**:1410−5.
175. Kauffman KJ, Dorkin JR, Yang JH, Heartlein MW, Derosa F, Mir FF, et al. Optimization of lipid nanoparticle formulations for mRNA delivery *in vivo* with fractional factorial and definitive screening designs. *Nano Lett* 2015;**15**:7300−6.
176. Taylor DD, Shah S. Methods of isolating extracellular vesicles impact down-stream analyses of their cargoes. *Methods* 2015;**87**:3−10.